Electronic Supplementary Material (ESI) for RSC Advances.

On-substrate **polymerization – a versatile approach for preparing conjugated polymers suitable as electrochromes and metal ion sensing**

Monika Wałęsa-Chorab[1] and W.G. Skene[1*]

[1]Laboratoire de caractérisation photophysique des matériaux conjugués
Département de chimie
Université de Montréal
CP 6128, Centre-ville
Montreal, QC

Corresponding author: w.skene@umontreal.ca

Tables of Contents

Figure S1. Spectroelectrochemistry of **P1** with applied voltages of 2000 (**—**), 1900 (**—**), 1800 (**—**), 1700 (**—**), 1500 (**—**), 1000 (**—**) and 100 (**—**) mV for 30 sec. 4

Figure S2. Percent transmission of **P1** monitored at 690 nm with switching potentials of 1500 and 100 mV for 40 and 5 sec. 5

Figure S3. Cyclic voltammograms of **P1** (**—**), **P2** (**—**), **P3** (**—**), **P4** (**—**), **P5** (**—**), **P6** (**—**) and **P7** (**—**)....6

Figure S4. Dependence of i_{ox} on the thickness of the layer of **P1**. 7

Figure S5. Dependence of i_{rev} on the thickness of the layer for **P1**. 8

Figure S6. Dependence of Δ*i* on the thickness of the layer of **P1**. 9

Figure S7. Dependence of i_{ox}/i_{rev} on the thickness of the layer of **P1 (**R = -0.92). 10

Figure S8. Dependence of ΔE on the thickness of the layer of **P1**. 11

Figure S9. Profilometry trace of **P1** immobilized on glass having a thickness of 1500 nm. 12

Figure S10. Profilometry trace of **P1** immobilized on glass having a thickness of 1000 nm. 13

Figure S11. Profilometry trace of **P1** immobilized on glass having a thickness of 750 nm. 14

Figure S12. Profilometry trace of **P1** immobilized on glass having a thickness of 500 nm. 15

Figure S13. Profilometry trace of **P1** immobilized on glass having a thickness of 350 nm. 16

Figure S14. Profilometry trace of **P1** immobilized on glass having a thickness of 130 nm. 17

Figure S15. Spectroelectrochemistry of **P2** with applied voltages of 0 (**—**), 800 (**—**), 1000 (**—**), 1100 (**—**), 1200 (**—**), 1300 (**—**), 1400 (**—**), and 1500 (**—**) mV for 30 sec. 18

Figure S16. Spectroelectrochemistry of **P2** with applied voltages of 1500 (**—**), 1400 (**—**), 1300 (**—**), 1200 (**—**), 1100 (**—**), 1000 (**—**), 800 (**—**), 600 (**—**), 400 (**—**), and 0 (**—**) mV for 30 sec 19

Figure S17. Transmission percent with switching potentials of 1300 and 100 mV for 20, 15, 10, 5 and 1 sec monitored at 720 nm for **P2**. 20

Figure S18. The UV-Vis spectra of polymer **P2** in its original (**—**), oxidized (**—**) and neutral (**—**) states. ..21

Figure S19. Dependence of cyclic voltammograms on the thickness of the layer of **P2** immobilized on ITO glass slides: 2000 (**—**), 1500 (**—**), 900 (**—**), 500 (**—**), 400 (**—**), 280 (**—**) and 130 (**—**) nm measured in anhydrous deaerated acetonitrille with 0.1 M $TBAPF_6$. 22

Figure S20. Dependence of i_{ox} on the thickness of the layer for **P2** (R = 0.96). 23

Figure S21. Dependence of i_{rev} on the thickness of the layer for **P2** (R = -0.96). 24

Figure S22. Dependence of Δ*i* on the thickness of the layer of **P2** (R = 0.96). 25

Figure S23. Dependence of i_{ox}/i_{rev} on the thickness of the layer of **P2**. 26

Figure S24. Dependence of ΔE on the thickness of the layer of **P2 (**R = 0.98). 27

Figure S25. Spectroelectrochemistry of **P3** with applied voltages of 0 (▬), 900 (▬),1000 (▬), 1100 (▬), 1200 (▬), 1300 (▬), 1400 (▬), 1500 (▬), 1600 (▬), 1700 (▬) and 1800 (▬) mV for 30 sec. 28

Figure S26. Spectroelectrochemistry of **P3** with applied voltages of 1800 (▬), 1600 (▬), 1400 (▬), 1200 (▬), 1000 (▬), 800 (▬), 600 (▬), and 0 (▬) mV for 30 sec. 29

Figure S27. Percent transmission of **P3** monitored at 700 nm with switching potentials of 1500 and 100 mV for 20, 15, 10, 5 and 1 sec. 30

Figure S28. Absorbance spectra of **P3** in its original (▬), oxidized (▬) and neutral (▬) states. 31

Figure S29. Dependence of cyclic voltammograms on the thickness of the layer of **P3** immobilized on ITO glass slides: 2500 (▬), 1000 (▬), 720 (▬), 400 (▬), 300 (▬), 200 (▬) and 120 (▬) nm measured in anhydrous degased acetonitrlle with 0.1 M $TBAPF_6$. 32

Figure S30. Dependence of i_{ox} on the thickness of the layer for **P3**. 33

Figure S31. Dependence of i_{rev} on the thickness of the layer for **P3** 34

Figure S32. Dependence of Δ*i* on the thickness of the layer of **P3**. 35

Figure S33. Dependence of i_{ox}/i_{rev} on the thickness of the layer of **P3**...36

Figure S34. Dependence of ΔE on the thickness of the layer of **P3**. 37

Figure S35. Complexation of **P1** (top), **P2** (middle) and **P3** (bottom) with various transition metal ions before (left) and after heating at 65ºC for 2h (right). 38

Figure S36. Corresponding legend of metal ion complexes drop-casted onto polymers from Figure 29...38

Figure S37. Absorbance spectra of complexes of **P1** immobilized on ITO coated glass with drop-cast $Cu(BF_4)_2$ (▬), $Cu(ClO_4)_2$ (▬),$Cu(OAc)_2$ (▬), $ZnCl_2$ (▬), $Zn(OTf)_2$ (▬), $Zn(ClO_4)_2$ (▬), $RuCl_3$ (▬), $Fe(BF_4)_2$ (▬), $Fe(OTf)_2$ (▬), $FeBr_3$ (▬), $Fe(ClO_4)_3$ (▬), $Co(ClO_4)_2$ (▬), $CoCl_2$ (▬), $AgBF_4$ (▬), $AgPF_6$ (▬), $EuCl_3$ (▬), $Ni(NO_3)_2$ (▬), CuI (▬), $Pb(OAc)_2$ (▬) and $Hg(OAc)_2$ (▬) measured after heating at 65ºC for 2h. 39

Table S1. Absorbance maximum of **P3** immobilized on ITO coated glass with various metal salts. 39

Table S2. Dependence of anodic cyclic voltammograms on the thickness of the layer of **P1**. 40

Table S3. Dependence of cyclic voltammograms on the thickness of the layer of **P2**. 40

Table S4. Dependence of cyclic voltammograms on the thickness of the layer of **P3**. 40

Figure S38. ^{1}H NMR spectrum of **1**. 41

Figure S39. ^{13}C NMR spectrum of **1**. 42

Figure S40 ^{1}H NMR spectrum of **2**. 43

Figure S41. ^{13}C NMR spectrum of **2**. 44

Figure S42. ^{1}H NMR spectrum of **3**. 45

Figure S43 ^{13}C NMR spectrum of **3**. 46

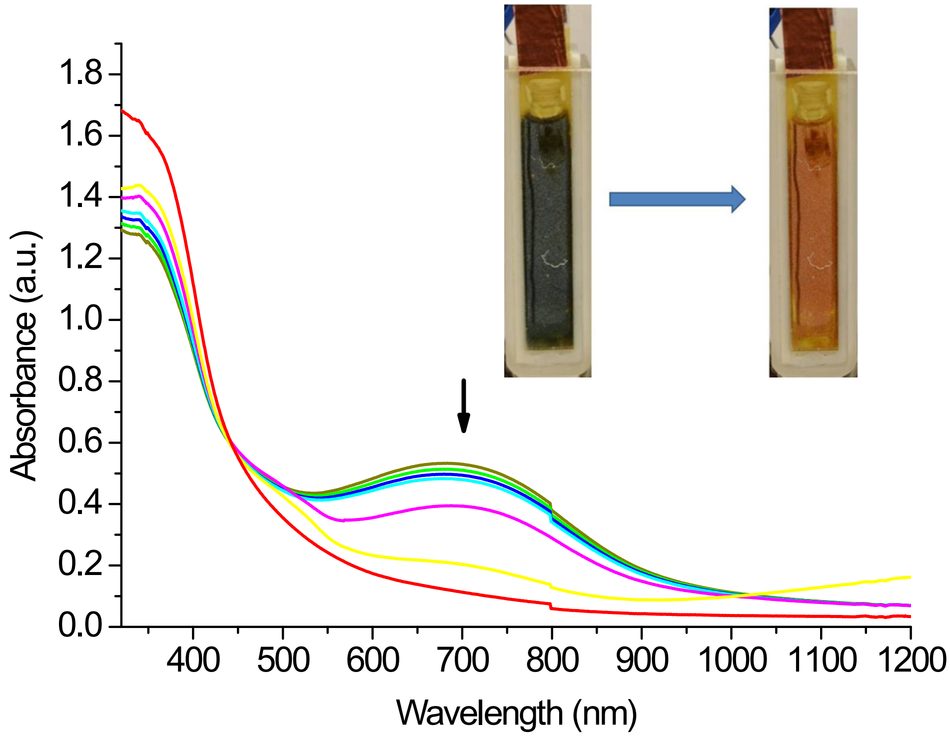

Figure S1. Spectroelectrochemistry of **P1** with applied voltages of 2000 (━), 1900 (━), 1800 (━), 1700 (━), 1500 (━), 1000 (━) and 100 (━) mV for 30 sec.

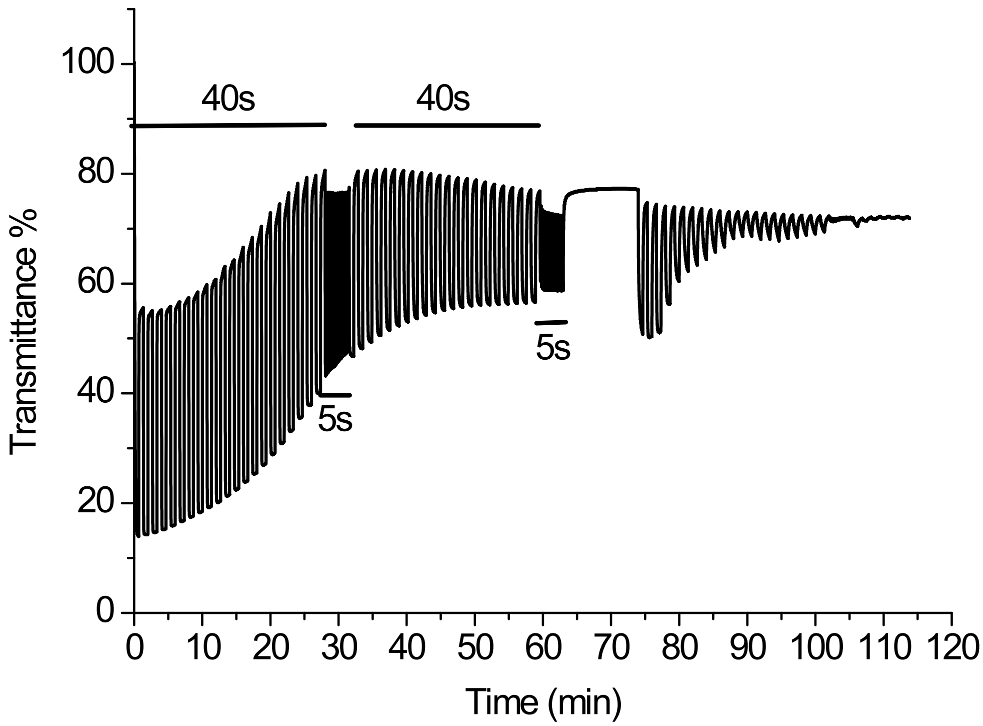

Figure S2. Percent transmission of **P1** monitored at 690 nm with switching potentials of 1500 and 100 mV for 40 and 5 sec.

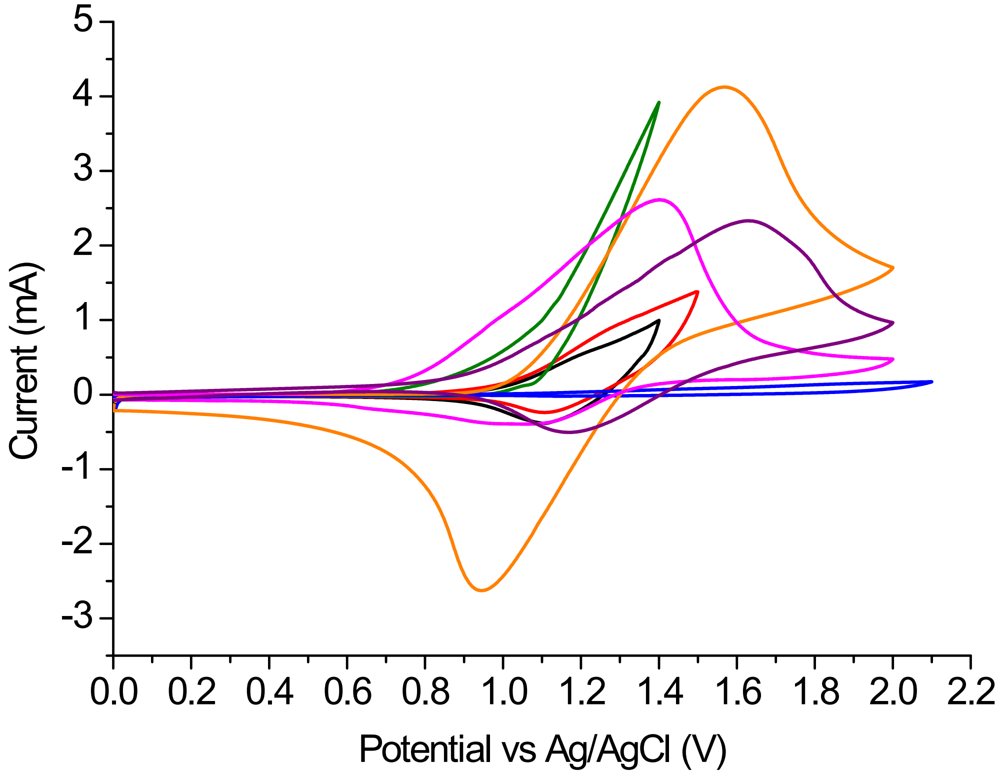

Figure S3. Cyclic voltammograms of **P1** (▬), **P2** (▬), **P3** (▬), **P4** (▬), **P5** (▬), **P6** (▬) and **P7** (▬).

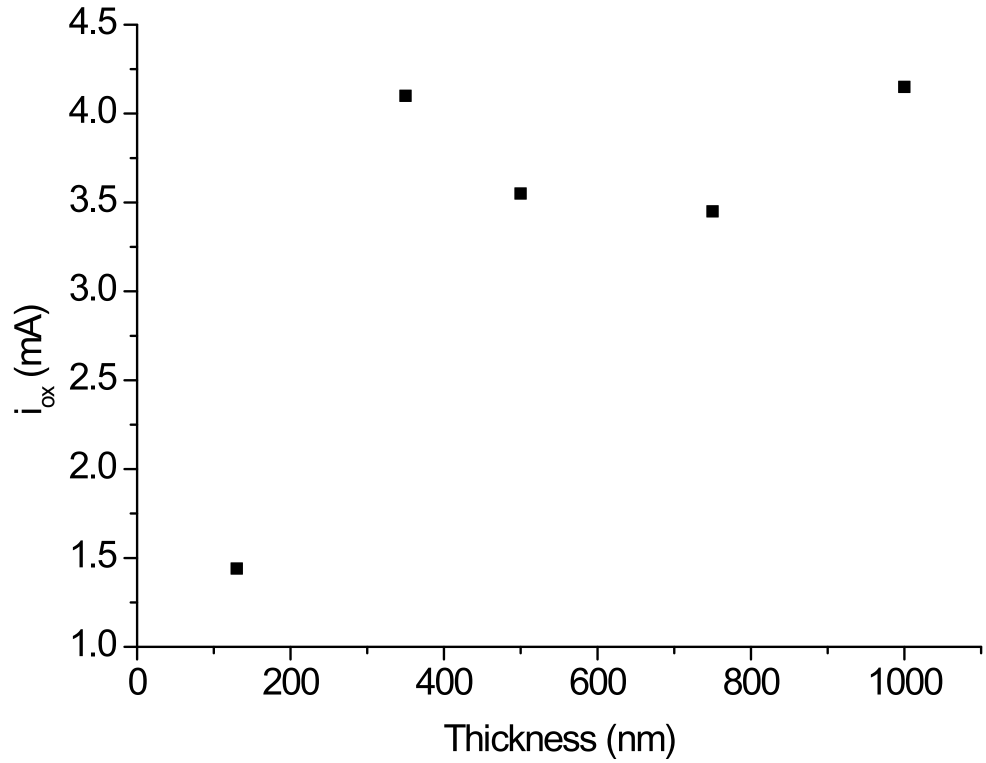

Figure S4. Dependence of i_{ox} on the thickness of the layer of **P1**.

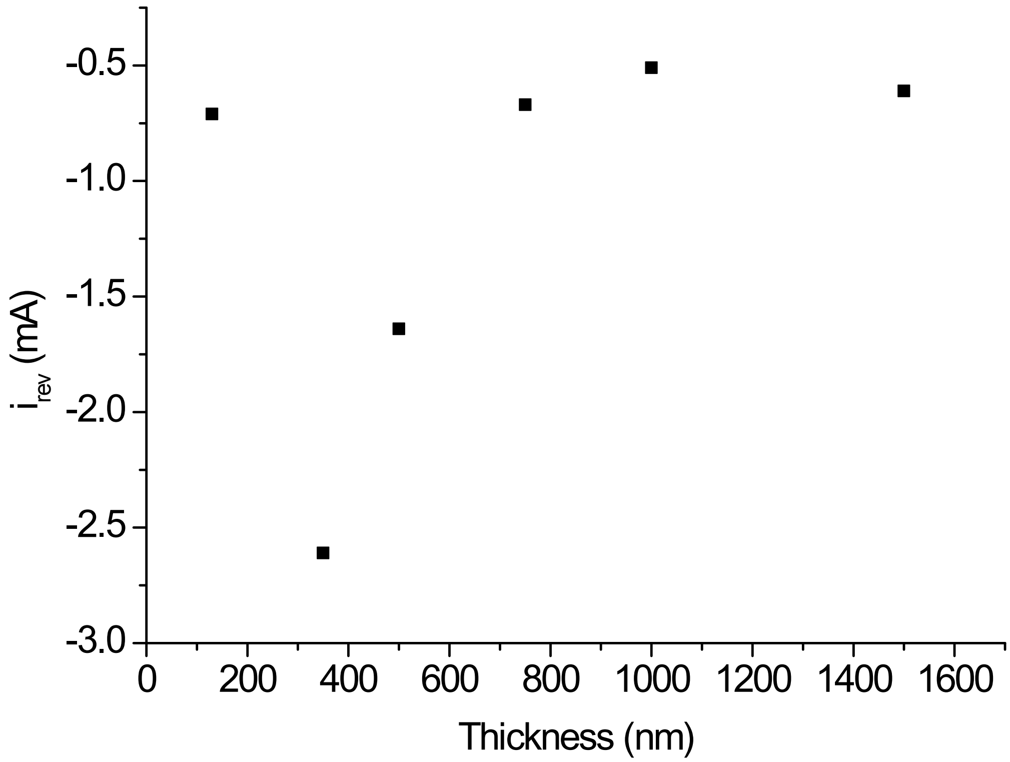

Figure S5. Dependence of i_{rev} on the thickness of the layer for **P1**.

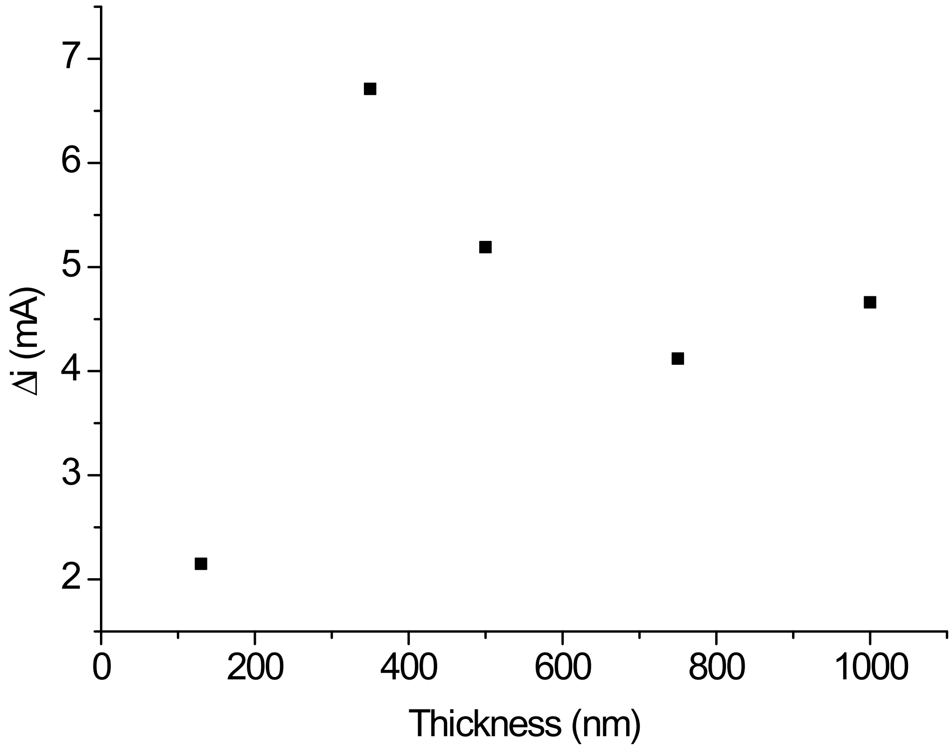

Figure S6. Dependence of Δi on the thickness of the layer of **P1**.

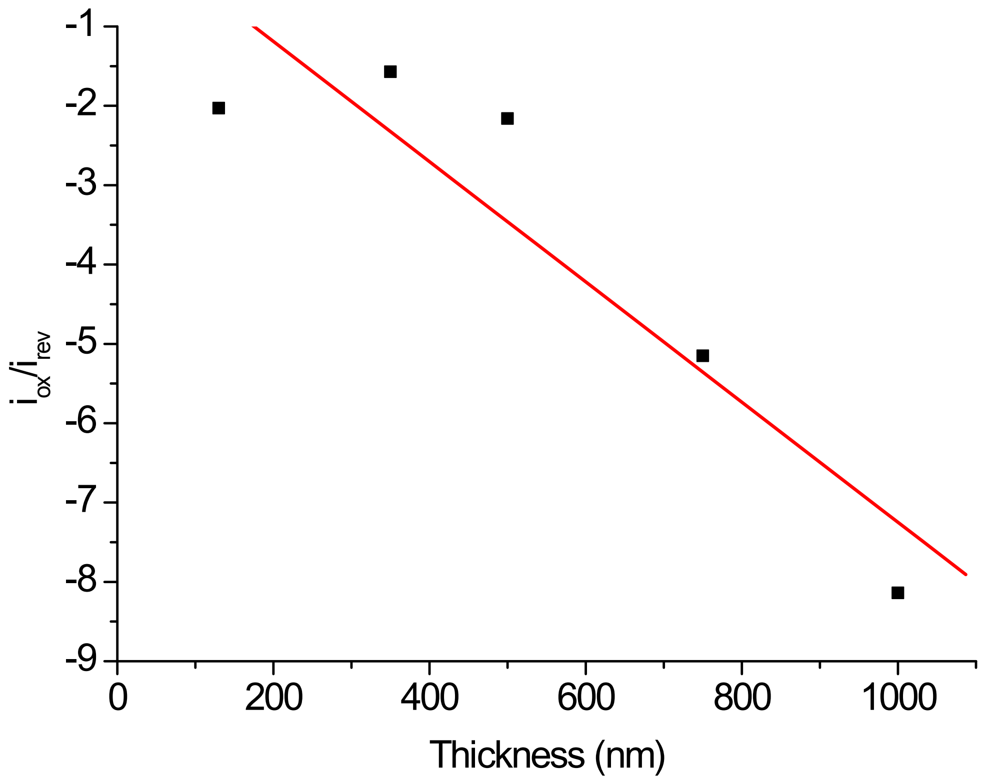

Figure S7. Dependence of i_{ox}/i_{rev} on the thickness of the layer of **P1 (**R = -0.92).

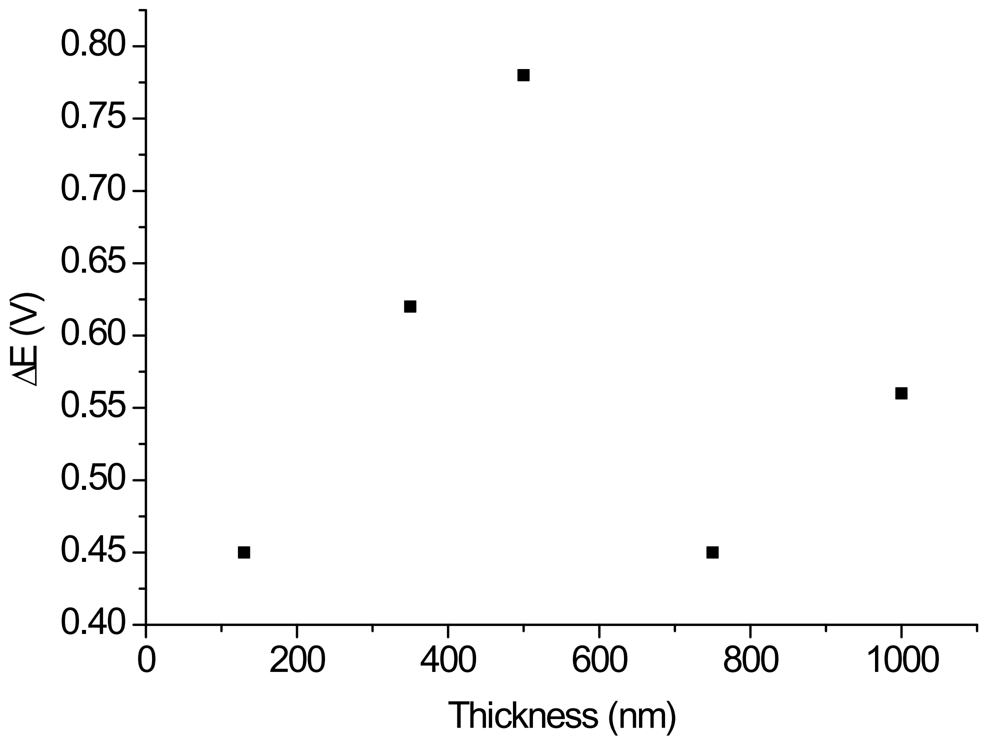

Figure S8. Dependence of ΔE on the thickness of the layer of **P1**.

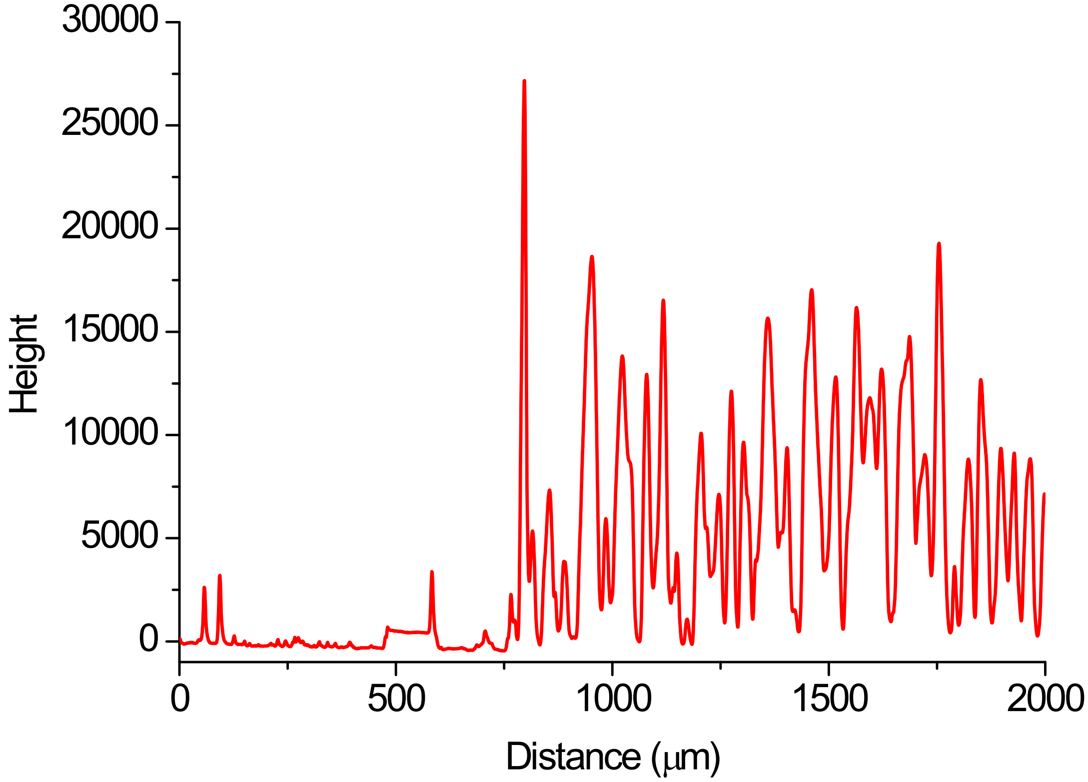

Figure S9. Profilometry trace of **P1** immobilized on glass having a thickness of 1500 nm.

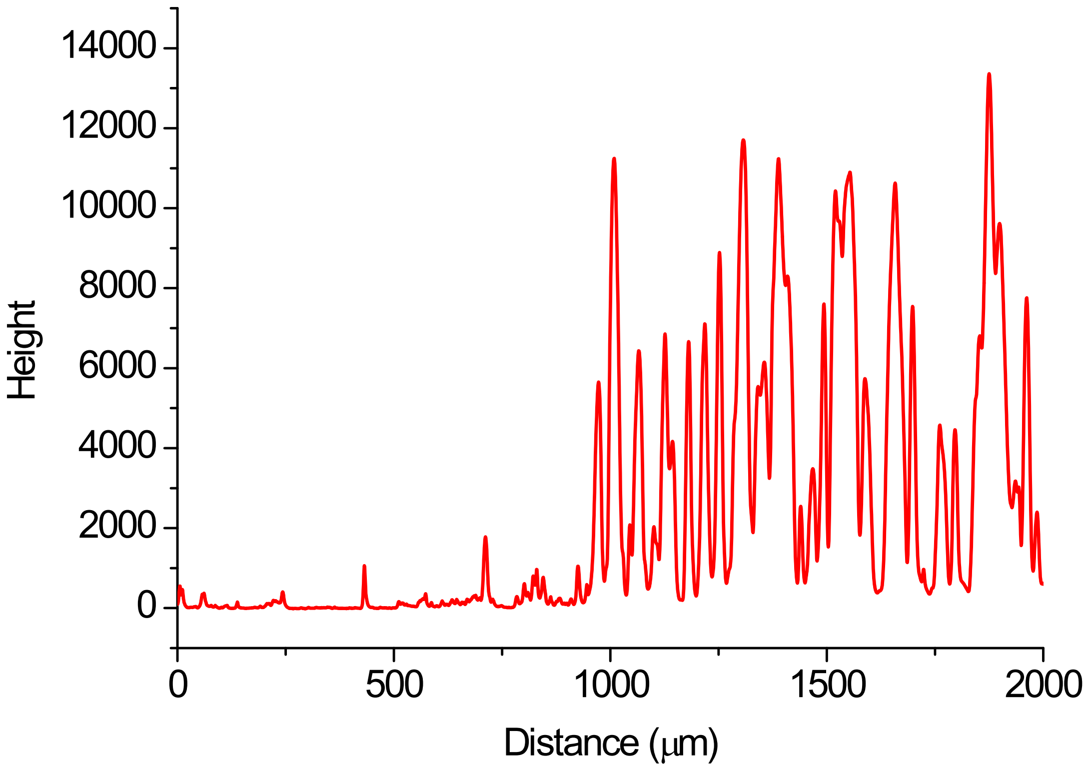

Figure S10. Profilometry trace of **P1** immobilized on glass having a thickness of 1000 nm.

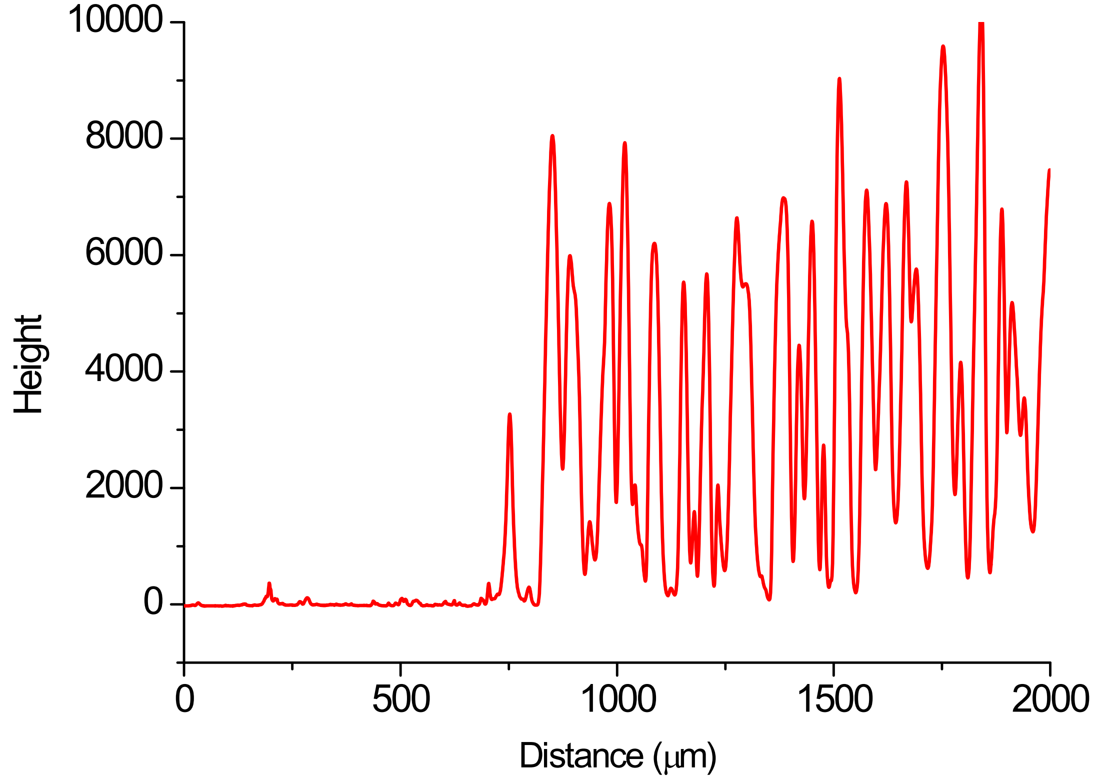

Figure S11. Profilometry trace of **P1** immobilized on glass having a thickness of 750 nm.

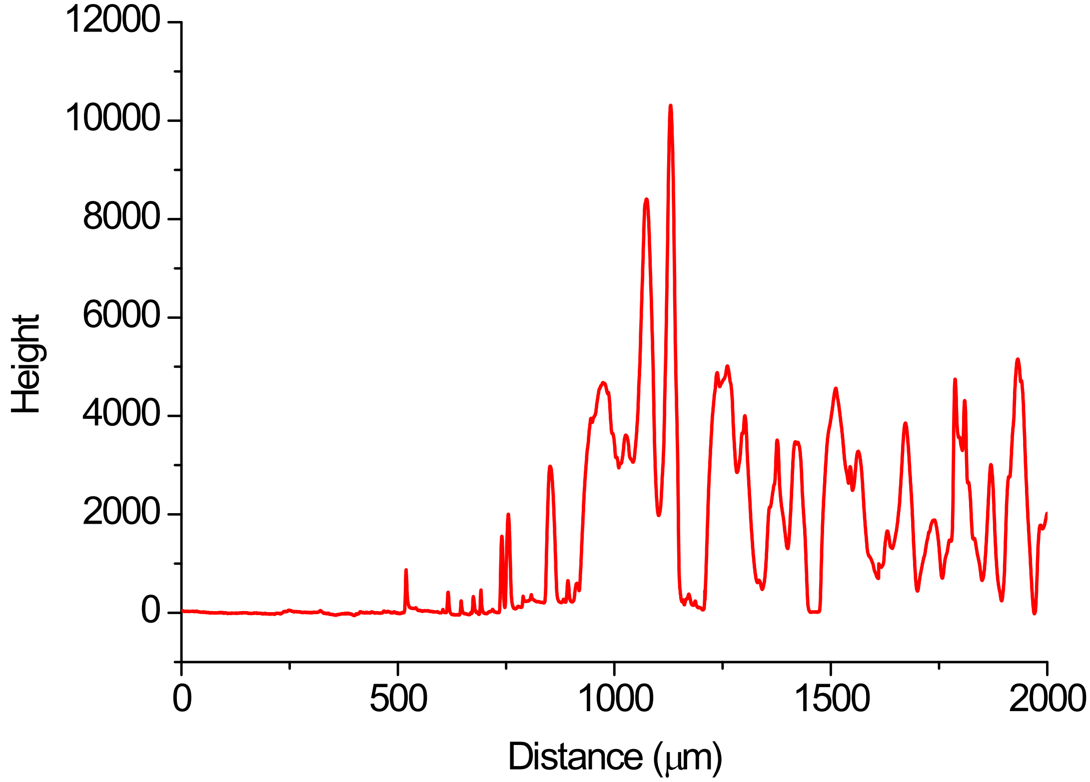

Figure S12. Profilometry trace of **P1** immobilized on glass having a thickness of 500 nm.

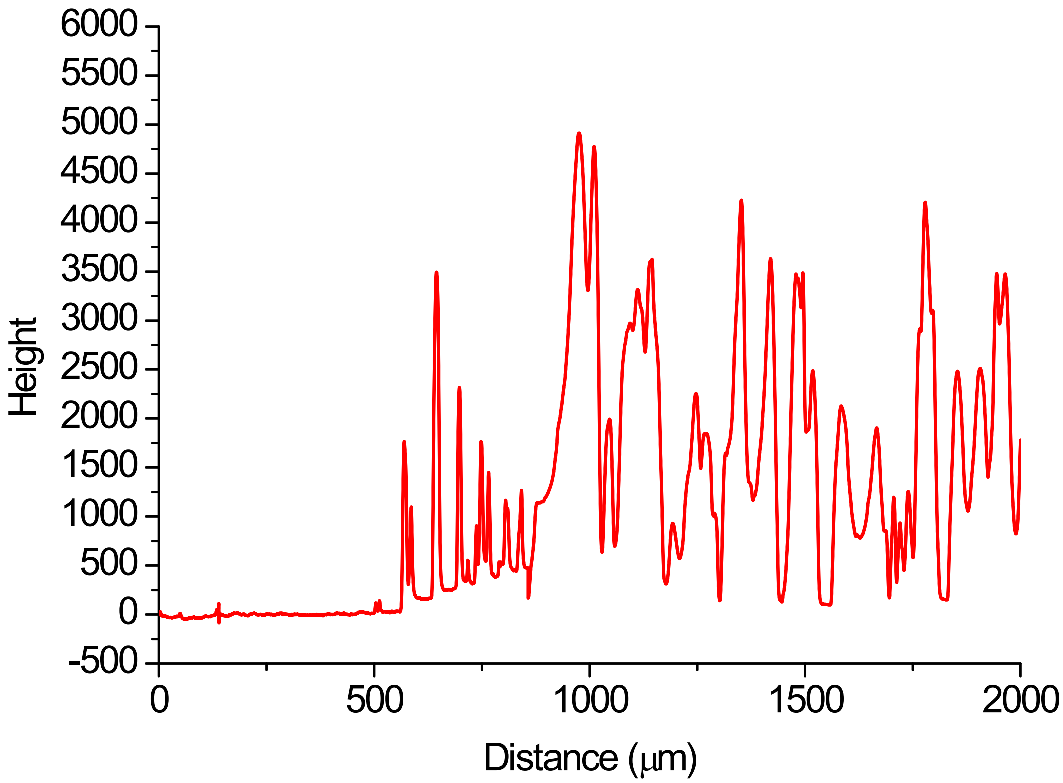

Figure S13. Profilometry trace of **P1** immobilized on glass having a thickness of 350 nm.

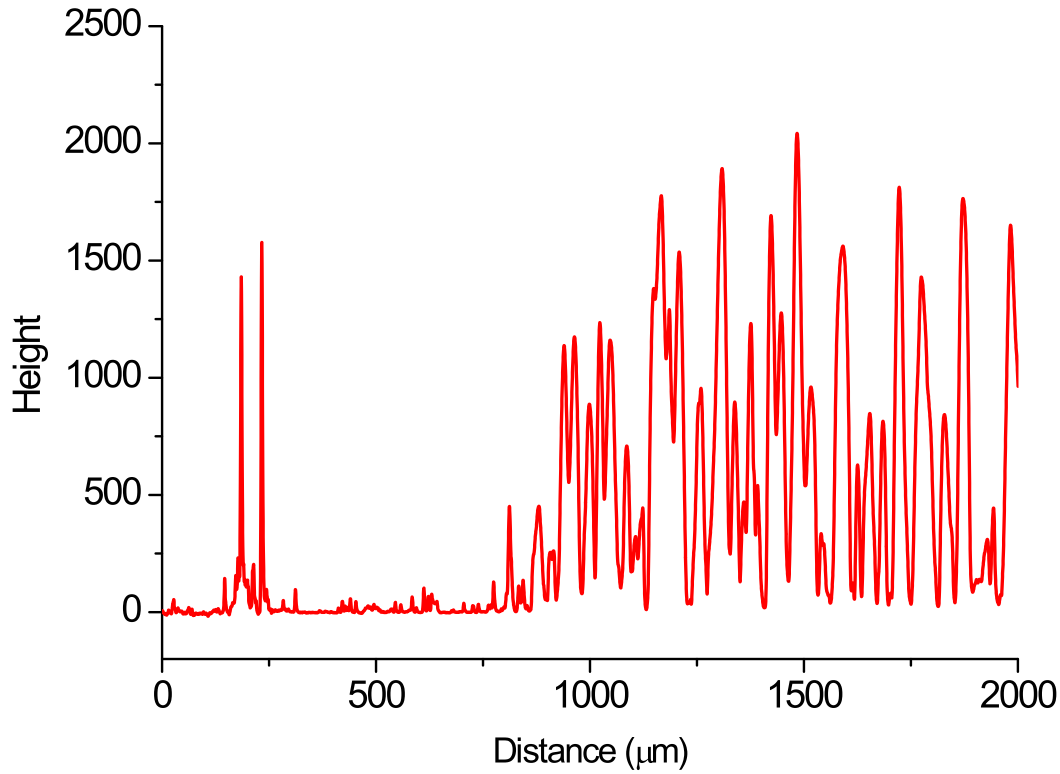

Figure S14. Profilometry trace of **P1** immobilized on glass having a thickness of 130 nm.

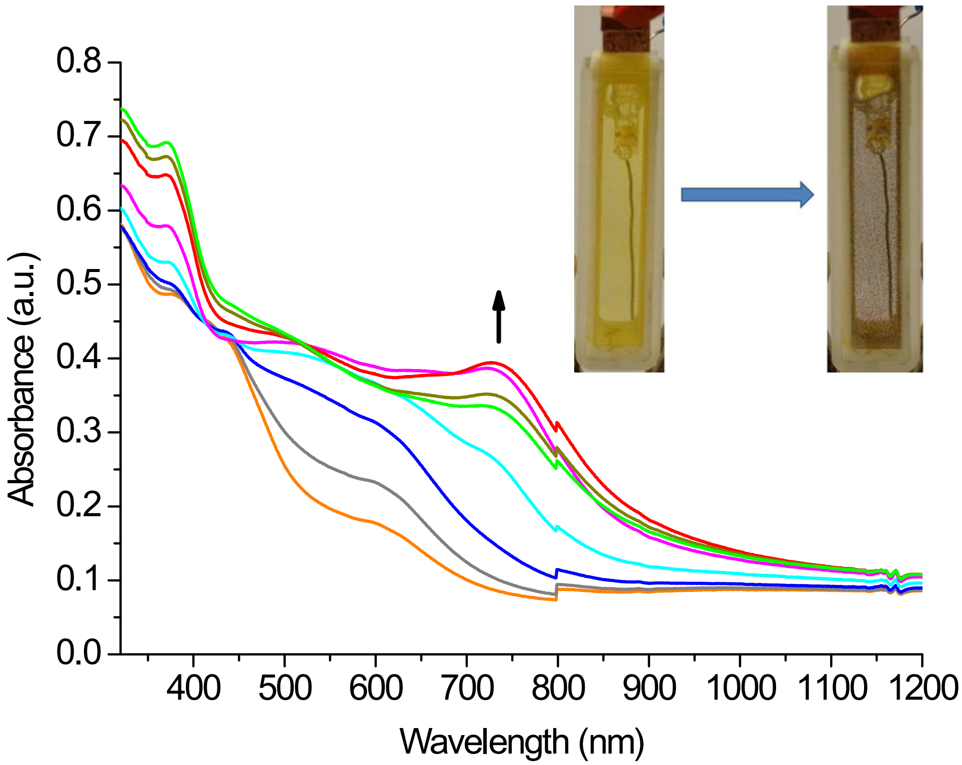

Figure S15. Spectroelectrochemistry of **P2** with applied voltages of 0 (—), 800 (—), 1000 (—), 1100 (—), 1200 (—), 1300 (—), 1400 (—), and 1500 (—) mV for 30 sec.

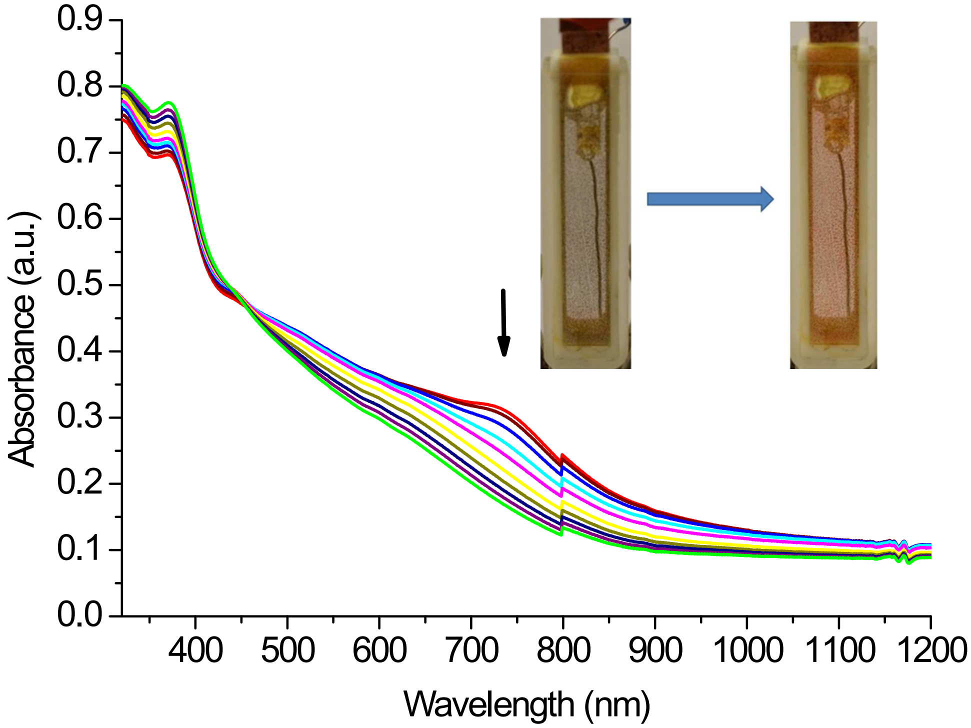

Figure S16. Spectroelectrochemistry of **P2** with applied voltages of 1500 (—), 1400 (—), 1300 (—), 1200 (—), 1100 (—), 1000 (—), 800 (—), 600 (—), 400 (—), and 0 (—) mV for 30 sec

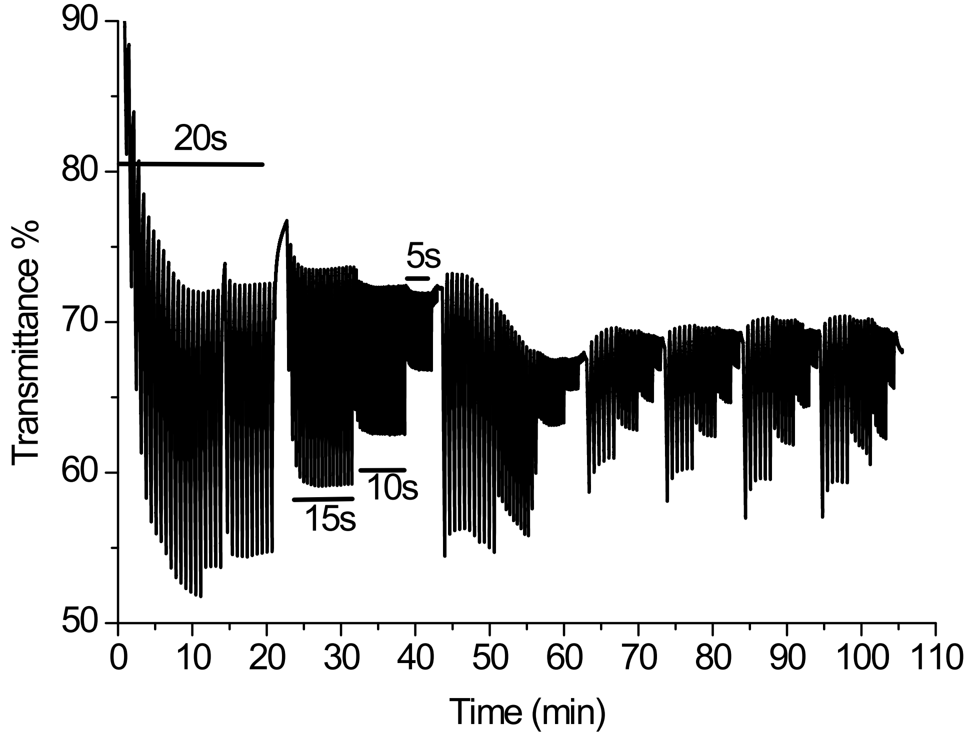

Figure S17. Transmission percent with switching potentials of 1300 and 100 mV for 20, 15, 10, 5 and 1 sec monitored at 720 nm for **P2**.

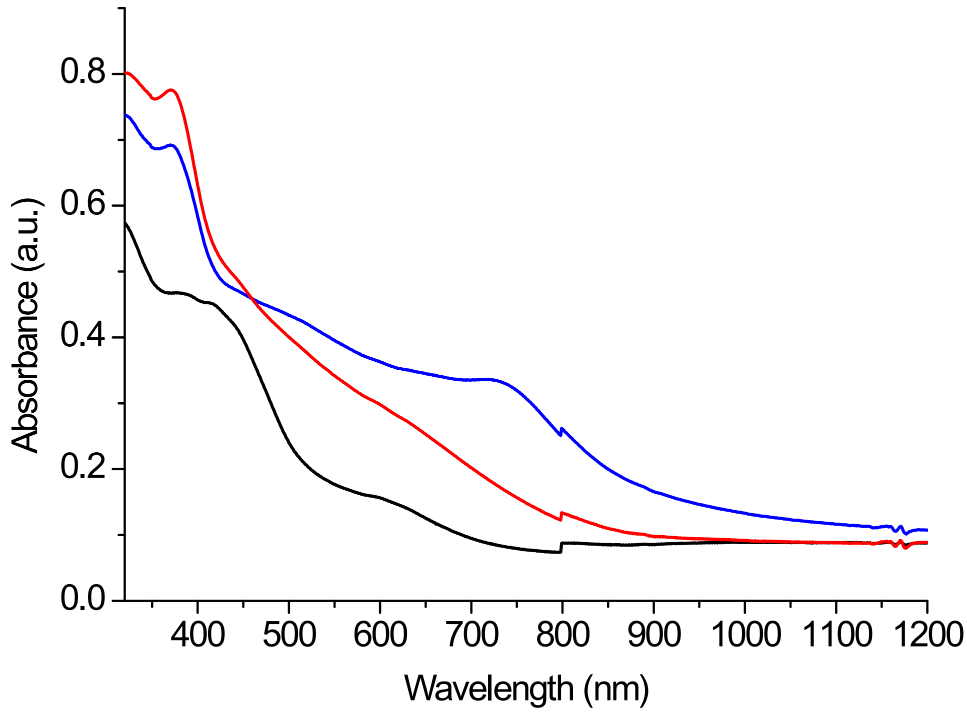

Figure S18. The UV-Vis spectra of polymer **P2** in its original (▬), oxidized (▬) and neutral (▬) states.

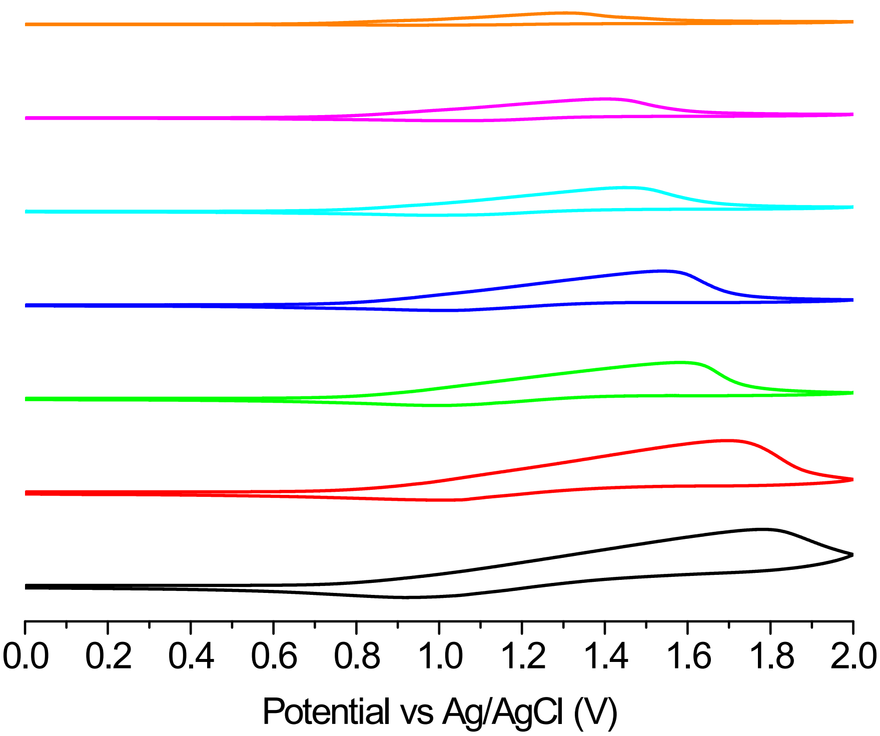

Figure S19. Dependence of cyclic voltammograms on the thickness of the layer of **P2** immobilized on ITO glass slides: 2000 (━), 1500 (━), 900 (━), 500 (━), 400 (━), 280 (━) and 130 (━) nm measured in anhydrous deaerated acetonitrille with 0.1 M $TBAPF_6$.

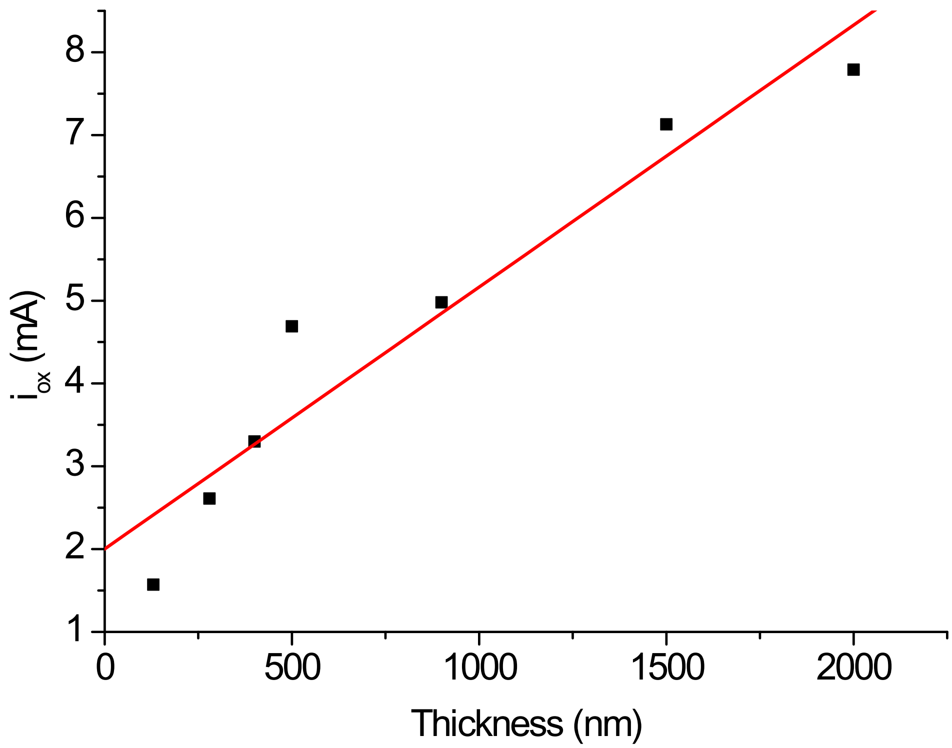

Figure S20. Dependence of i_{ox} on the thickness of the layer for **P2** (R = 0.96).

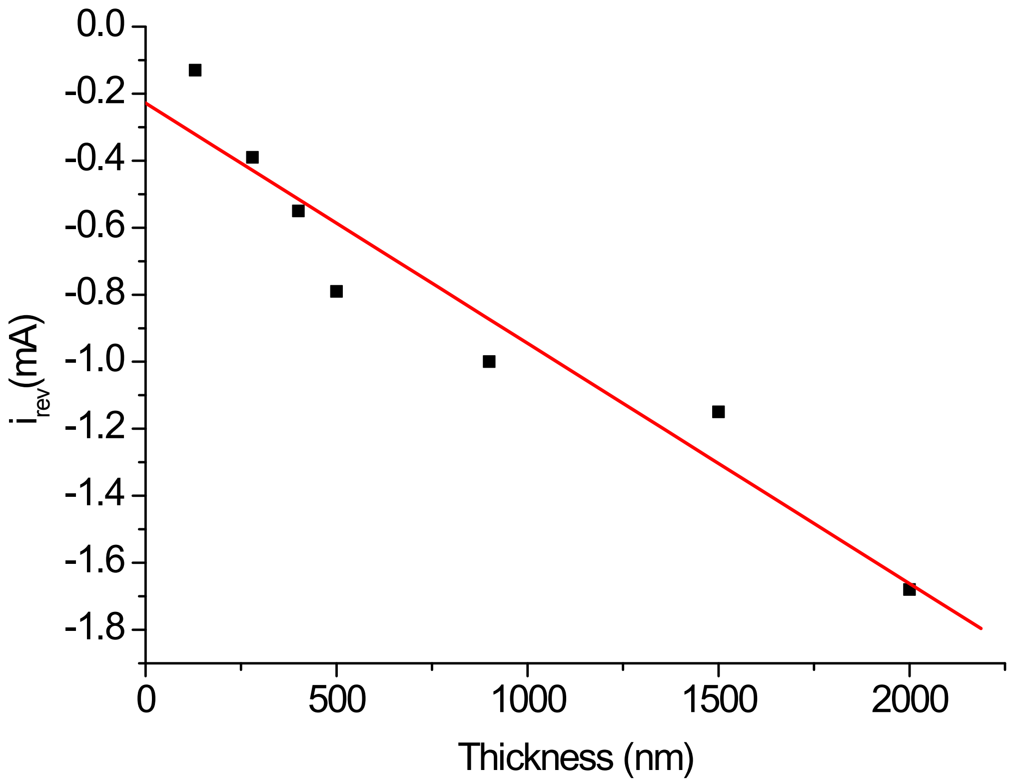

Figure S21. Dependence of i_{rev} on the thickness of the layer for **P2** (R = -0.96).

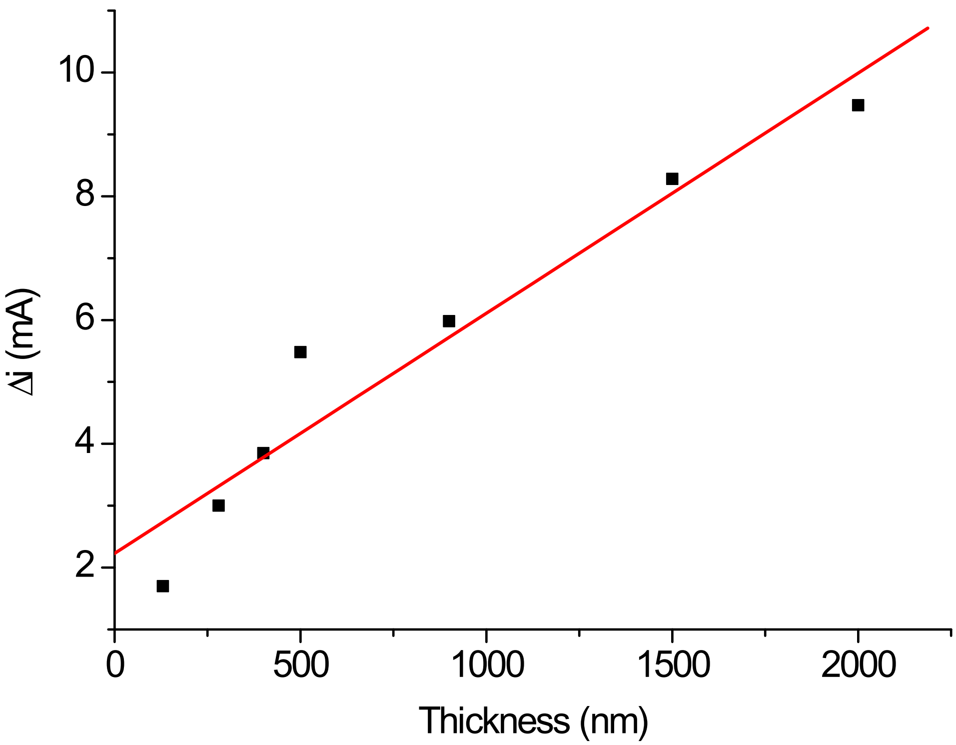

Figure S22. Dependence of Δ*i* on the thickness of the layer of **P2** (R = 0.96).

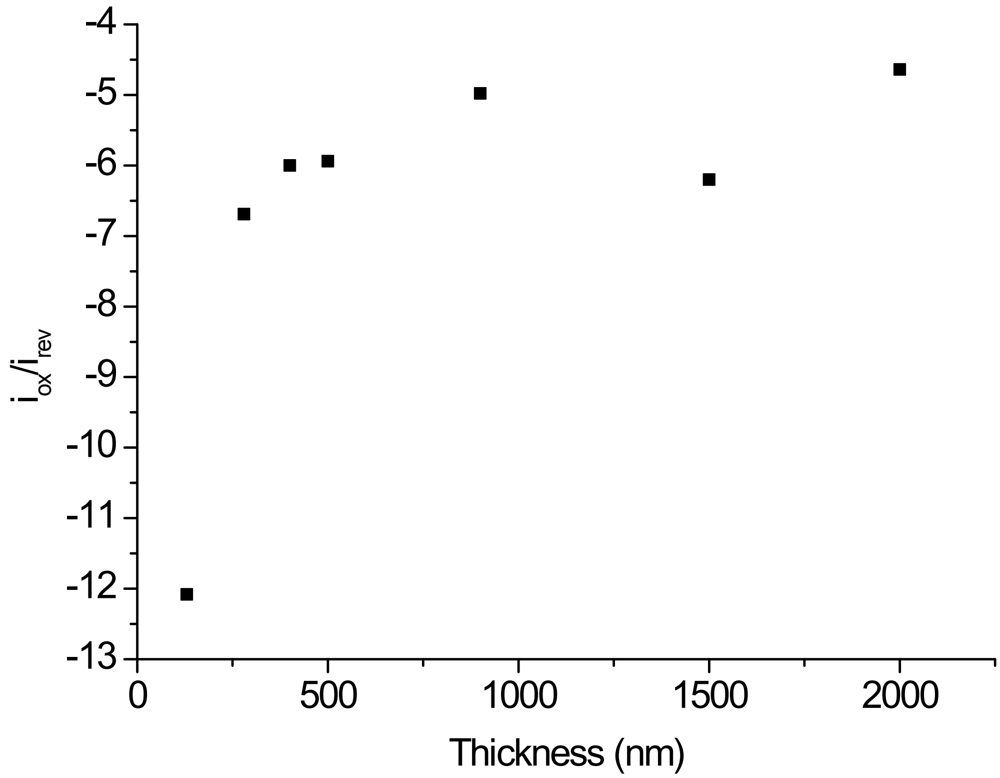

Figure S23. Dependence of i_{ox}/i_{rev} on the thickness of the layer of **P2**.

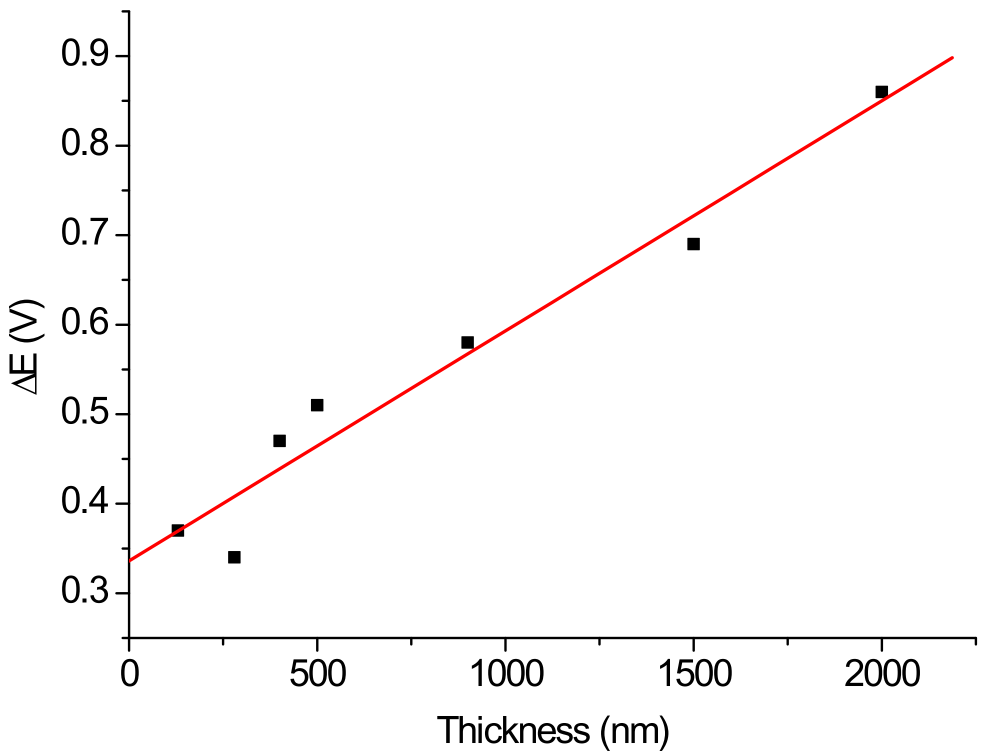

Figure S24. Dependence of ΔE on the thickness of the layer of **P2 (**R = 0.98).

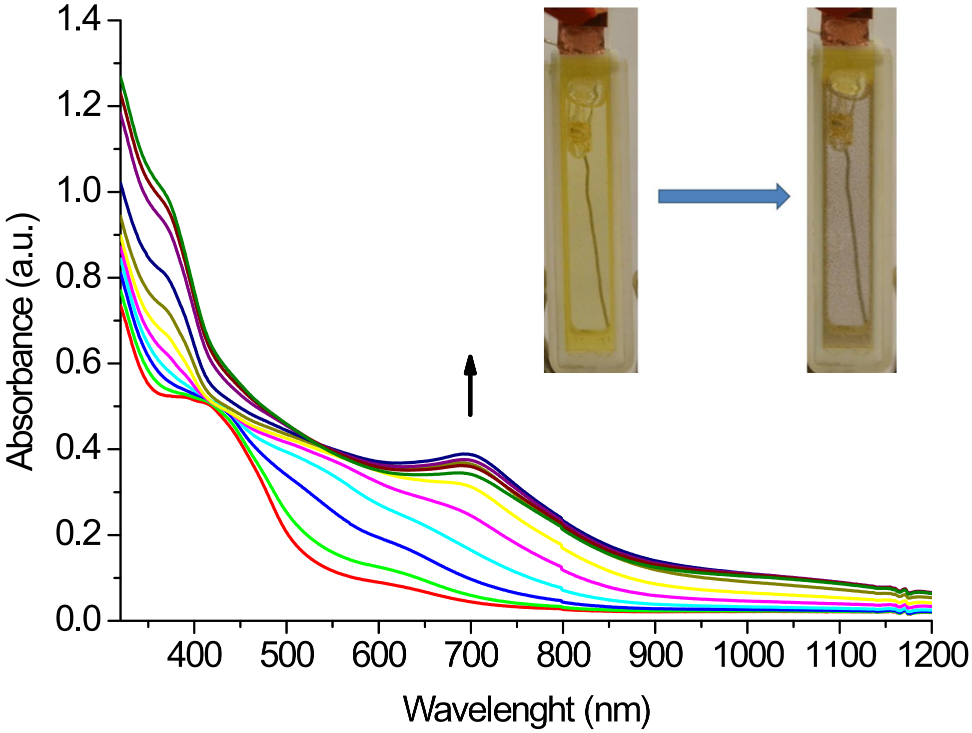

Figure S25. Spectroelectrochemistry of **P3** with applied voltages of 0 (—), 900 (—),1000 (—), 1100 (—), 1200 (—), 1300 (—), 1400 (—), 1500 (—), 1600 (—), 1700 (—) and 1800 (—) mV for 30 sec.

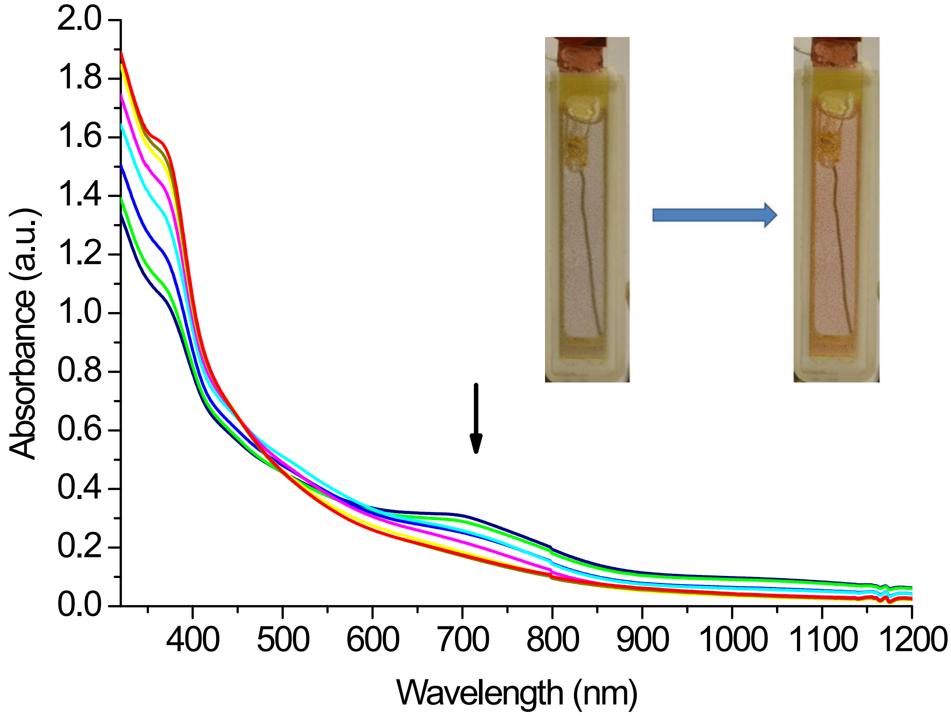

Figure S26. Spectroelectrochemistry of **P3** with applied voltages of 1800 (—), 1600 (—), 1400 (—), 1200 (—), 1000 (—), 800 (—), 600 (—), and 0 (—) mV for 30 sec.

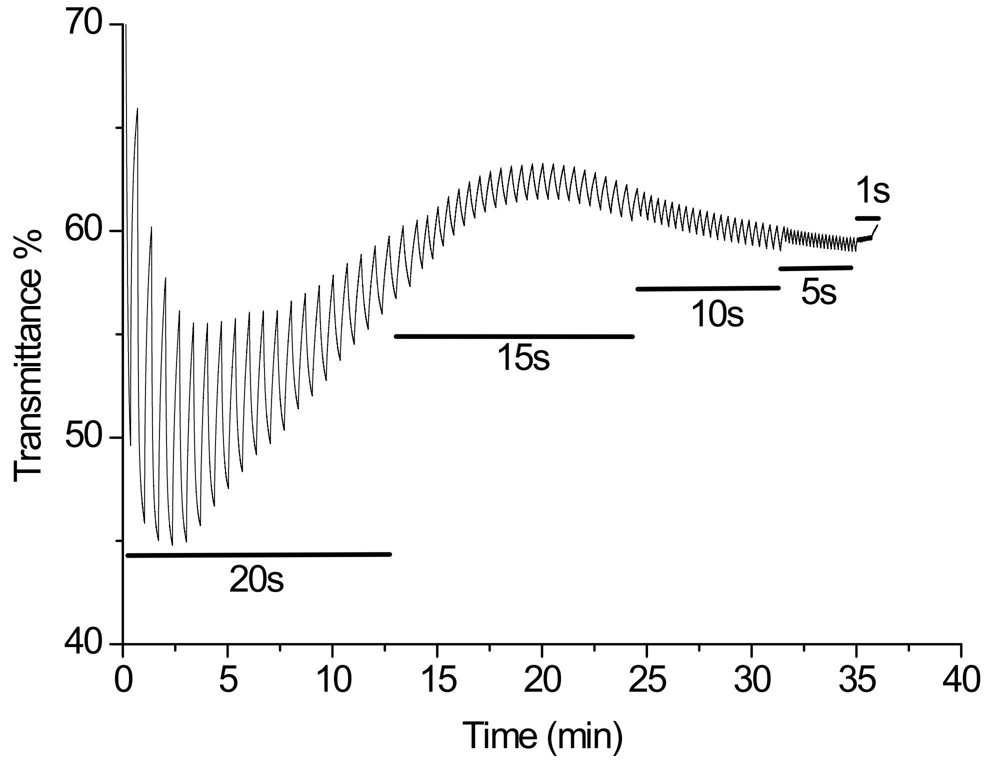

Figure S27. Percent transmission of **P3** monitored at 700 nm with switching potentials of 1500 and 100 mV for 20, 15, 10, 5 and 1 sec.

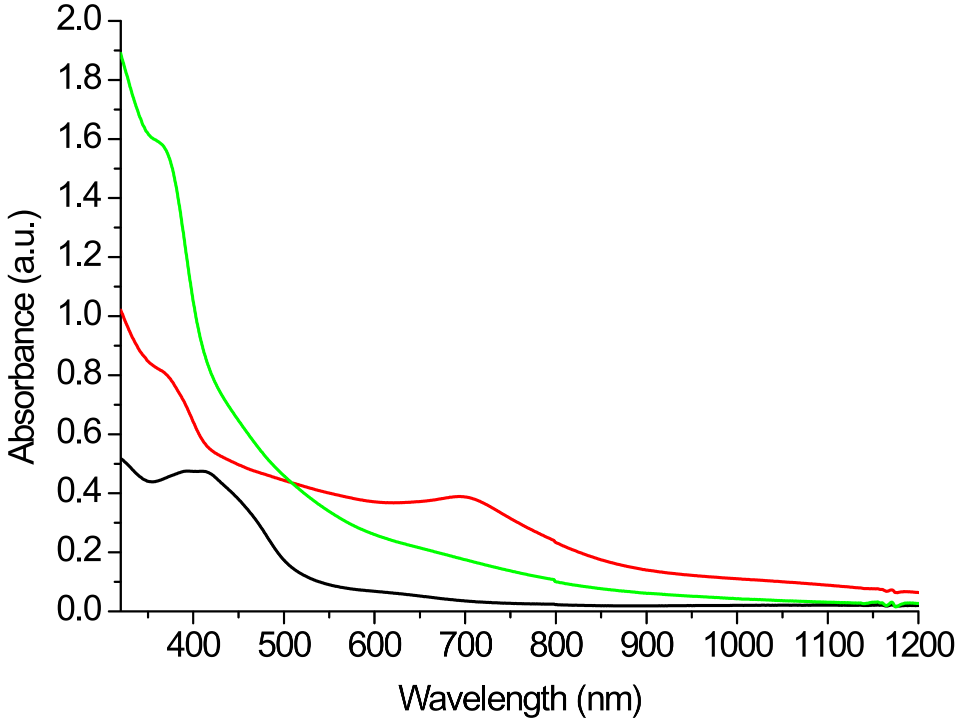

Figure S28. Absorbance spectra of **P3** in its original (▬), oxidized (▬) and neutral (▬) states.

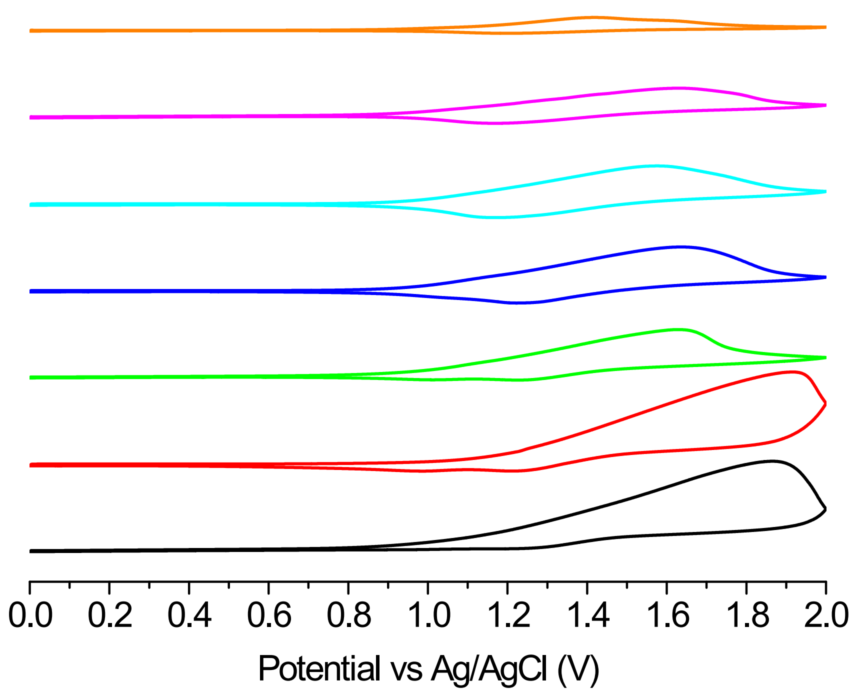

Figure S29. Dependence of cyclic voltammograms on the thickness of the layer of **P3** immobilized on ITO glass slides: 2500 (▬), 1000 (▬), 720 (▬), 400 (▬), 300 (▬), 200 (▬) and 120 (▬) nm measured in anhydrous degased acetonitrlle with 0.1 M $TBAPF_6$.

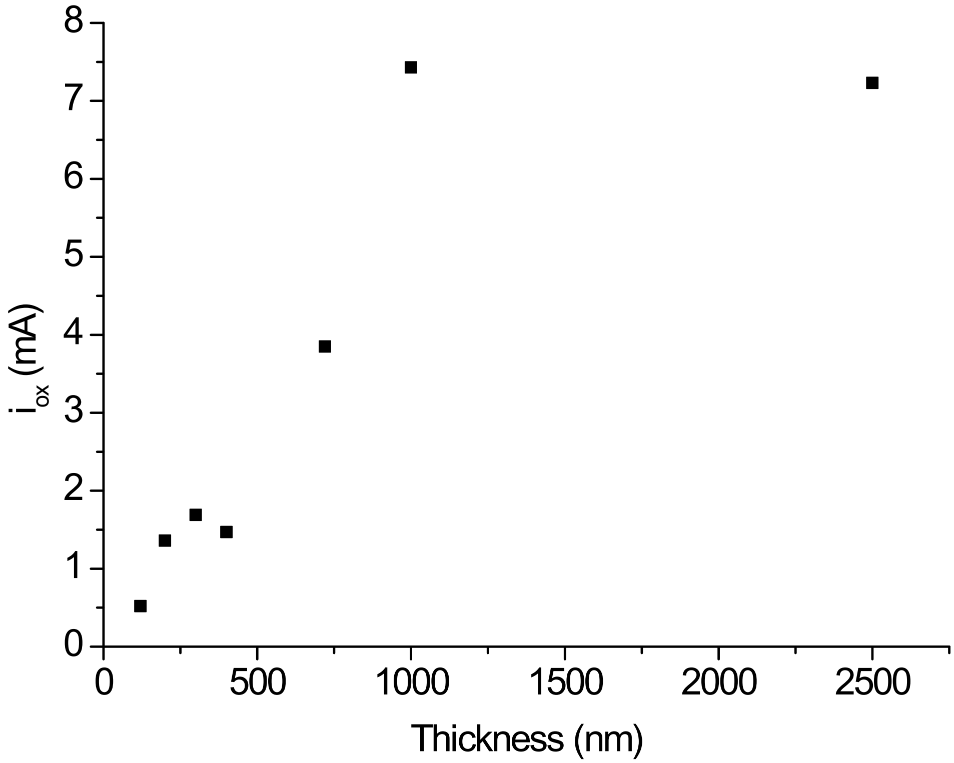

Figure S30. Dependence of i_{ox} on the thickness of the layer for **P3**.

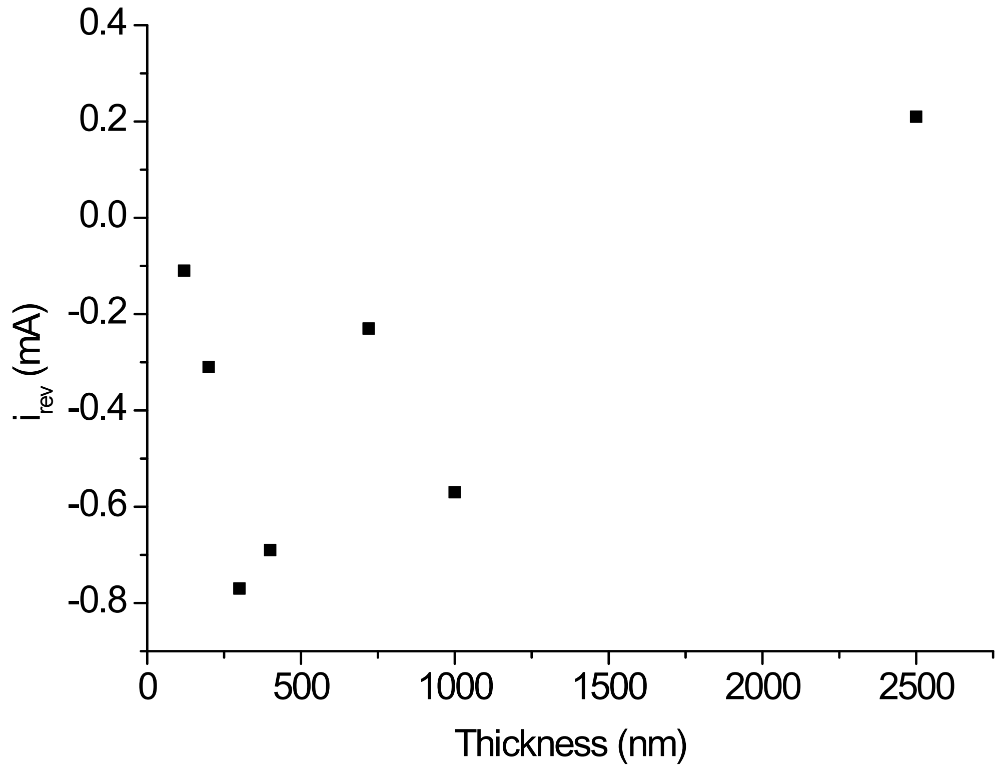

Figure S31. Dependence of i_{rev} on the thickness of the layer for **P3**

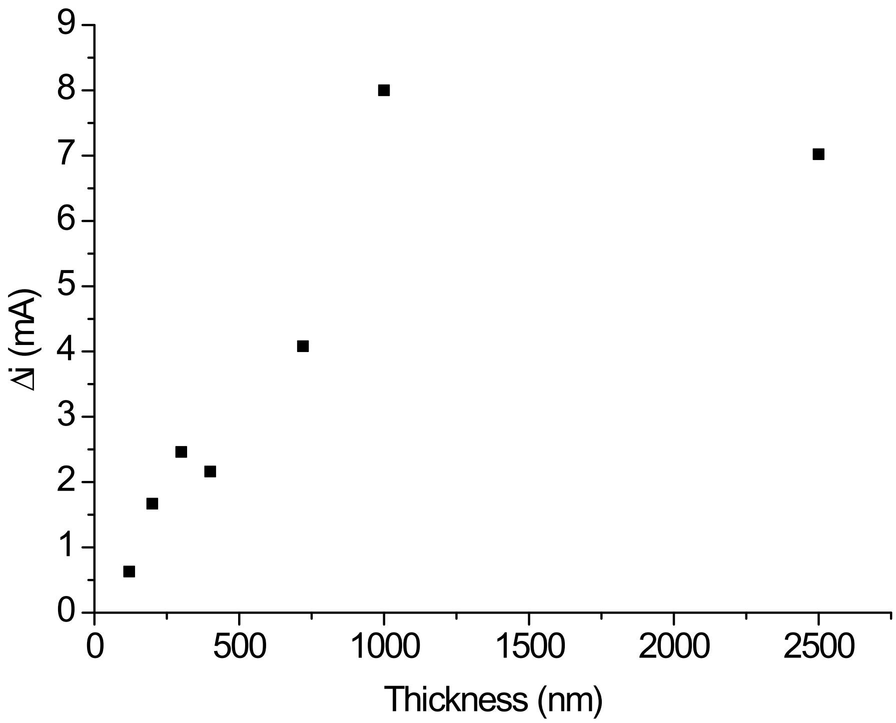

Figure S32. Dependence of Δ*i* on the thickness of the layer of **P3**.

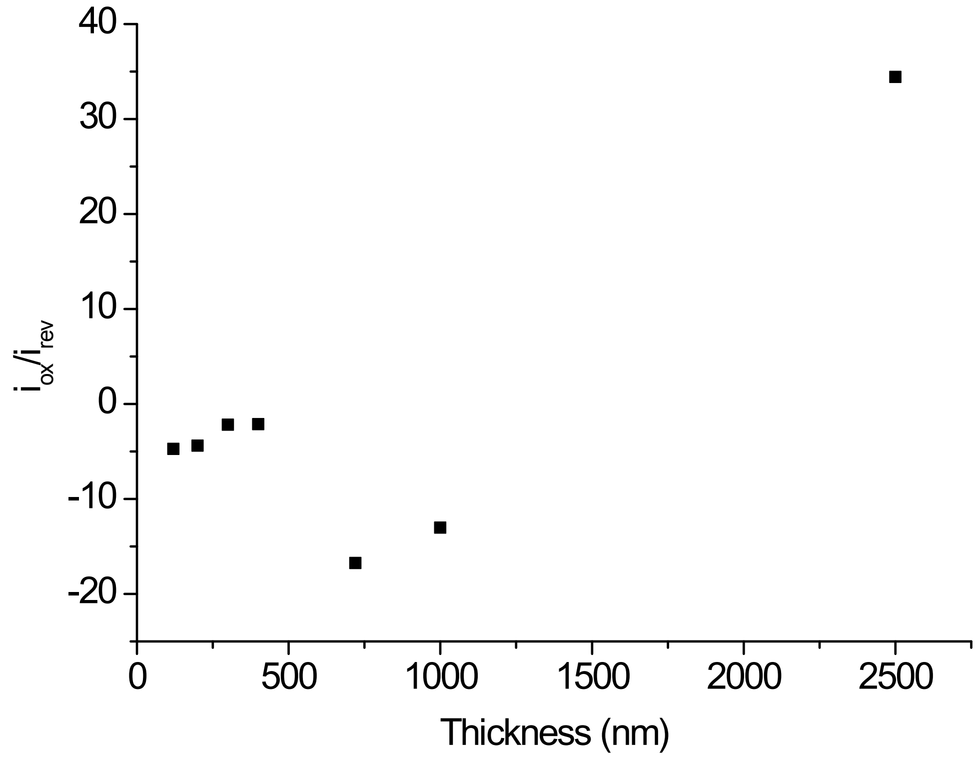

Figure S33. Dependence of i_{ox}/i_{rev} on the thickness of the layer of **P3**.

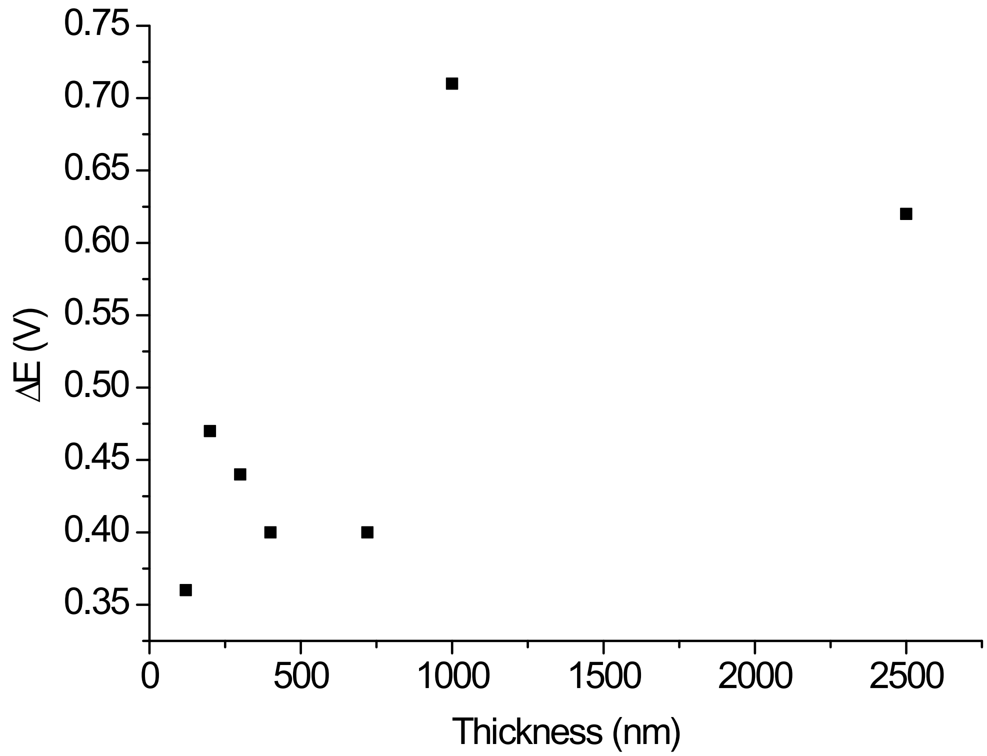

Figure S34. Dependence of ΔE on the thickness of the layer of **P3**.

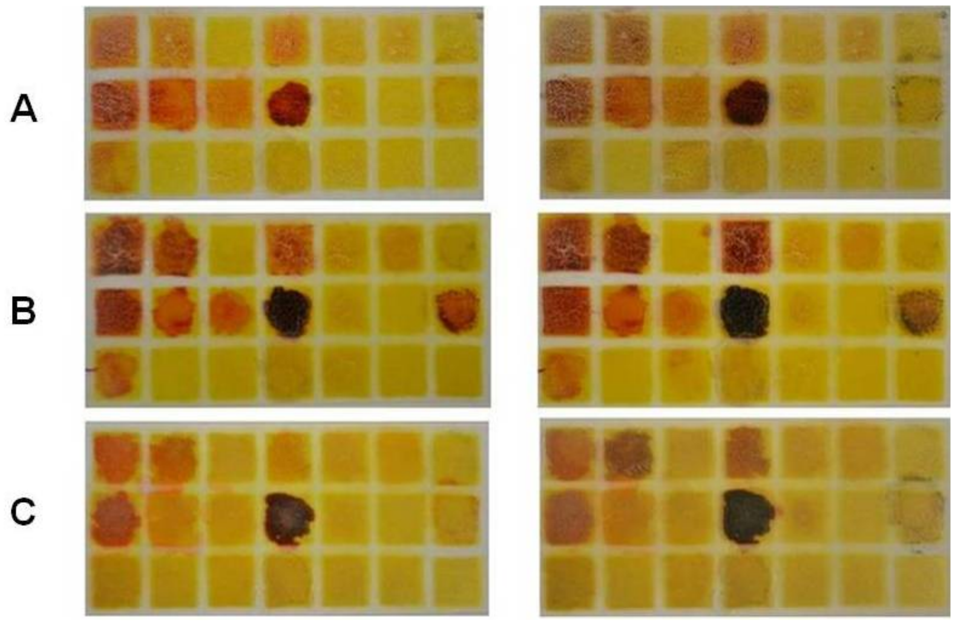

Figure S35. Complexation of **P1** (top), **P2** (middle) and **P3** (bottom) with various transition metal ions before (left) and after heating at 65ºC for 2h (right).

$Cu(BF_4)_2$	$Cu(ClO_4)_2$	$Cu(OAc)_2$	$ZnCl_2$	$Zn(CF_3SO_3)_2$	$Zn(ClO_4)_2$	$RuCl_3$
$Fe(BF_4)_2$	$Fe(CF_3SO_3)_3$	$FeBr_3$	$Fe(ClO_4)_3$	$Co(ClO_4)_2$	$CoCl_2$	$AgBF_4$
$AgPF_6$	$EuCl_3$	$Ni(NO_3)_2$	CuI	$Pb(OAc)_2$	$Hg(OAc)_2$	Original polymer

Figure S36. Corresponding legend of metal ion complexes drop-casted onto polymers from Figure 29.

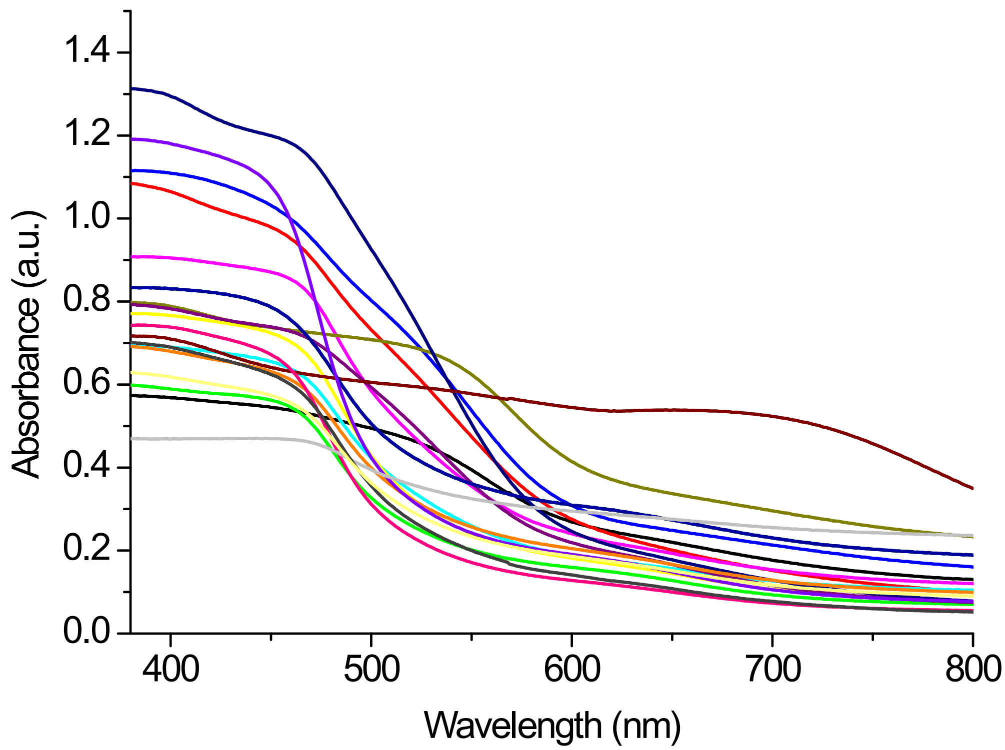

Figure S37. Absorbance spectra of complexes of **P1** immobilized on ITO coated glass with drop-cast $Cu(BF_4)_2$ (▬), $Cu(ClO_4)_2$ (▬),$Cu(OAc)_2$ (▬), $ZnCl_2$ (▬), $Zn(OTf)_2$ (▬), $Zn(ClO_4)_2$ (▬), $RuCl_3$ (▬), $Fe(BF_4)_2$ (▬), $Fe(OTf)_2$ (▬), $FeBr_3$ (▬), $Fe(ClO_4)_3$ (▬), $Co(ClO_4)_2$ (▬), $CoCl_2$ (▬), $AgBF_4$ (▬), $AgPF_6$ (▬), $EuCl_3$ (▬), $Ni(NO_3)_2$ (▬), CuI (▬), $Pb(OAc)_2$ (▬) and $Hg(OAc)_2$ (▬) measured after heating at 65ºC for 2h.

Table S1. Absorbance maximum of **P3** immobilized on ITO coated glass with various metal salts.

metal salt	λ_{abs} (nm)	metal salt	λ_{abs} (nm)	metal salt	λ_{abs} (nm)
$Cu(BF_4)_2$	504	$Fe(BF_4)_2$	535	$AgPF_6$	458
$Cu(ClO_4)_2$	459	$Fe(OTf)_2$	466	$EuCl_3$	439
$Cu(OAc)_2$	444	$FeBr_3$	468	$Ni(NO_3)_2$	452
$ZnCl_2$	451	$Fe(ClO_4)_3$	696	CuI	467
$Zn(OTf)_2$	460	$Co(ClO_4)_2$	442	$Pb(OAc)_2$	455
$Zn(ClO_4)_2$	460	$CoCl_2$	448	$Hg(OAc)_2$	458
$RuCl_3$	459	$AgBF_4$	445		

Table S2. Dependence of anodic cyclic voltammograms on the thickness of the layer of **P1**.

	i_{ox} (mA)	i_{rev} (mA)	Δi (mA)	i_{ox}/i_{rev}	E_{ox} (V)	E_{rev} (V)	ΔE (V)
1500 nm	-	-0.61	-	-	-	1.40	-
1000 nm	4.15	-0.51	4.66	-8.14	1.70	1.14	0.56
750 nm	3.45	-0.67	4.12	-5.15	1.64	1.19	0.45
500 nm	3.55	-1.64	5.19	-2.16	1.83	1.05	0.78
350 nm	4.10	-2.61	6.71	-1.57	1.57	0.95	0.62
130 nm	1.44	-0.71	2.15	-2.03	1.50	1.05	0.45

Table S3. Dependence of cyclic voltammograms on the thickness of the layer of **P2**.

	i_{ox} (mA)	i_{rev} (mA)	Δi (mA)	i_{ox}/i_{rev}	E_{ox} (V)	E_{rev} (V)	ΔE (V)
2000 nm	7.79	-1.68	9.47	-4.64	1.78	0.92	0.86
1500 nm	7.13	-1.15	8.28	-6.20	1.70	1.01	0.69
900 nm	4.98	-1.00	5.98	-4.98	1.58	1.00	0.58
500 nm	4.69	-0.79	5.48	-5.94	1.54	1.03	0.51
400 nm	3.30	-0.55	3.85	-6.00	1.45	0.98	0.47
280 nm	2.61	-0.39	3.00	-6.69	1.40	1.06	0.34
130 nm	1.57	-0.13	1.70	-12.08	1.30	0.93	0.37

Table S4. Dependence of cyclic voltammograms on the thickness of the layer of **P3**.

	i_{ox} (mA)	i_{rev} (mA)	Δi (mA)	i_{ox}/i_{rev}	E_{ox} (V)	E_{rev} (V)	ΔE (V)
2500 nm	7.23	0.21	7.02	34.43	1.87	1.25	0.62
1000 nm	7.43	-0.57	8.00	-13.03	1.92	1.21	0.71
720 nm	3.85	-0.23	4.08	-16.74	1.63	1.23	0.40
400 nm	1.47	-0.69	2.16	-2.13	1.53	1.13	0.40
300 nm	1.69	-0.77	2.46	-2.19	1.52	1.08	0.44
200 nm	1.36	-0.31	1.67	-4.39	1.54	1.07	0.47
120 nm	0.52	-0.11	0.63	-4.73	1.40	1.04	0.36

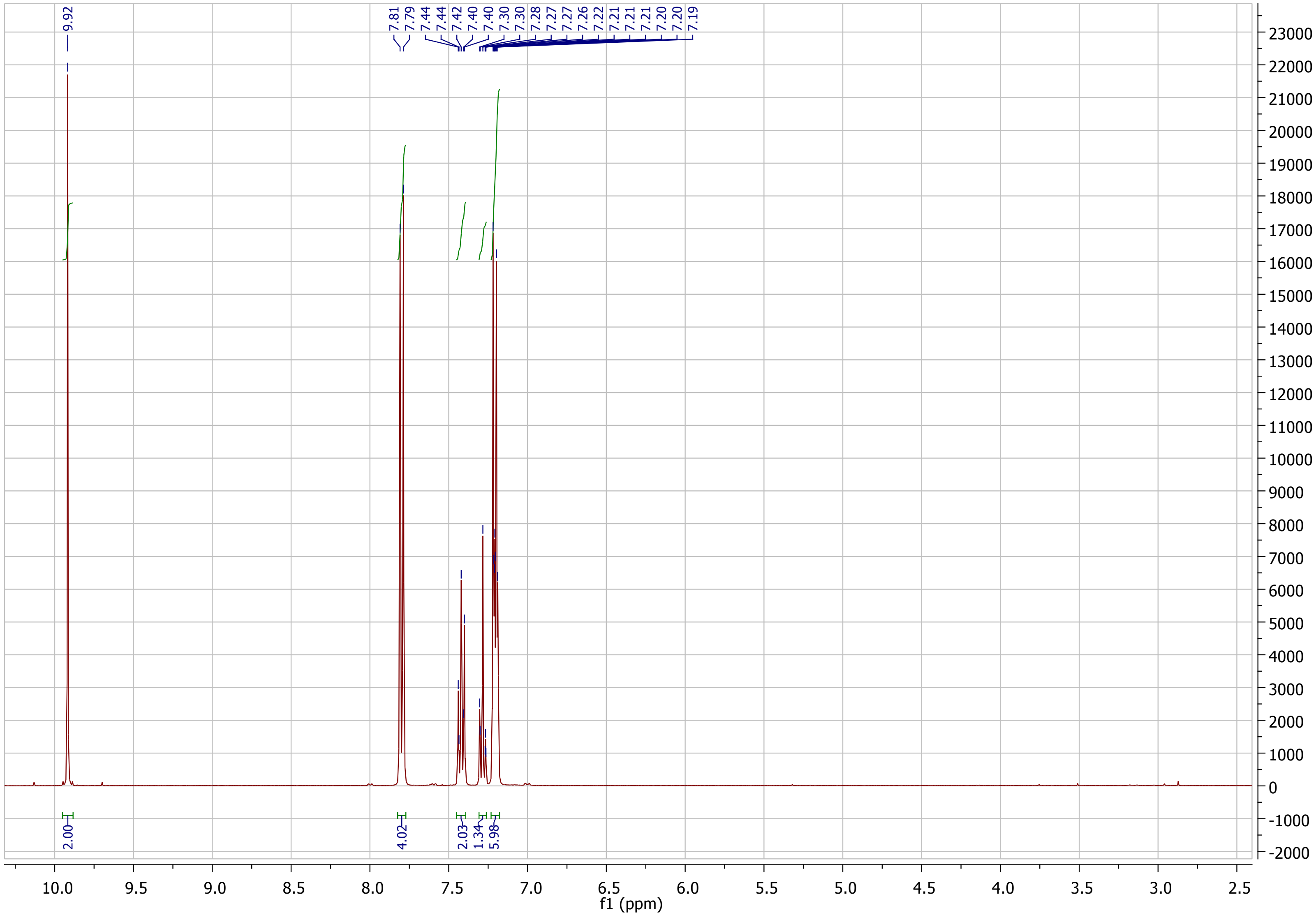

Figure S38. ^{1}H NMR spectrum of **1**.

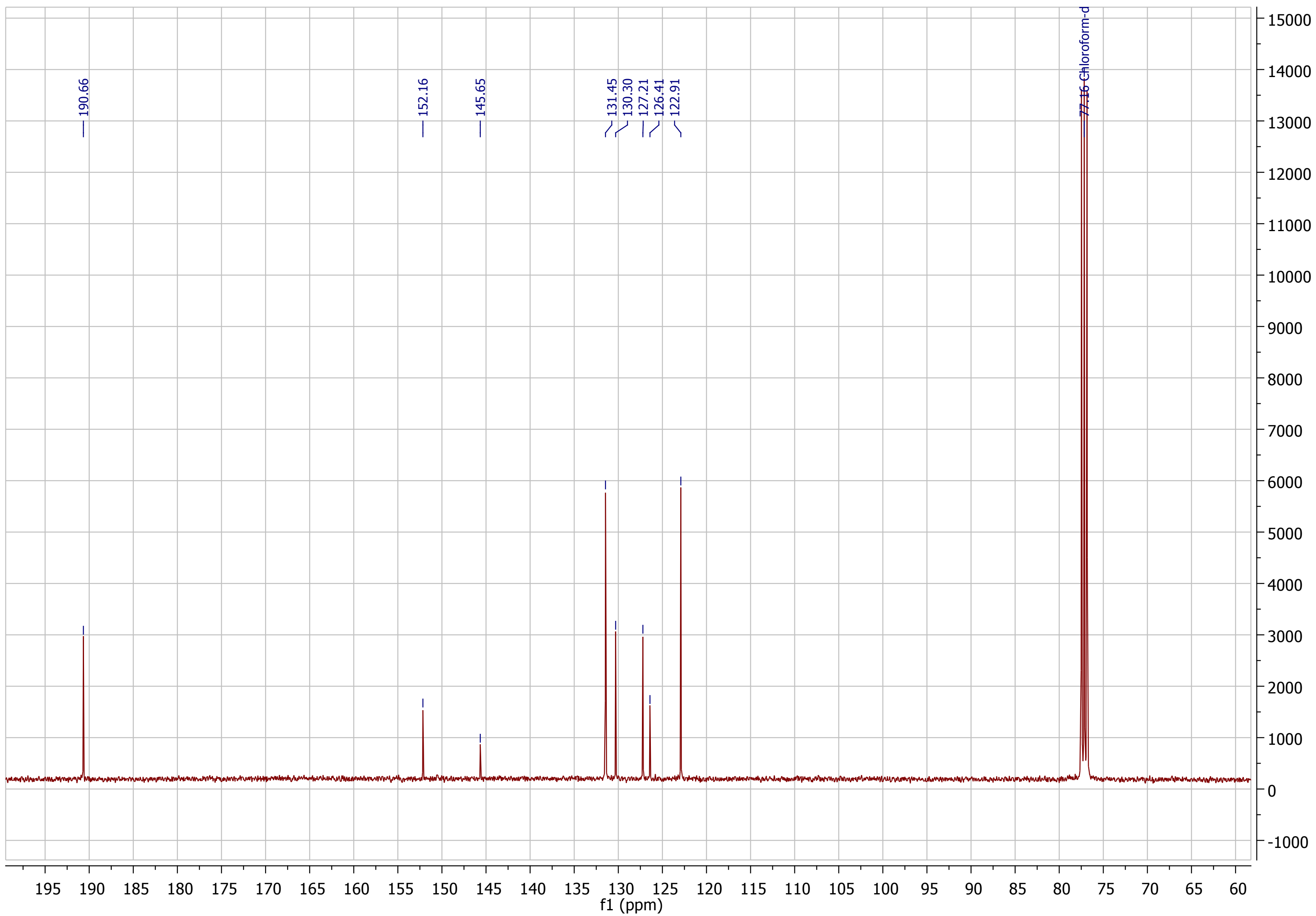

Figure S39. ^{13}C NMR spectrum of **1**.

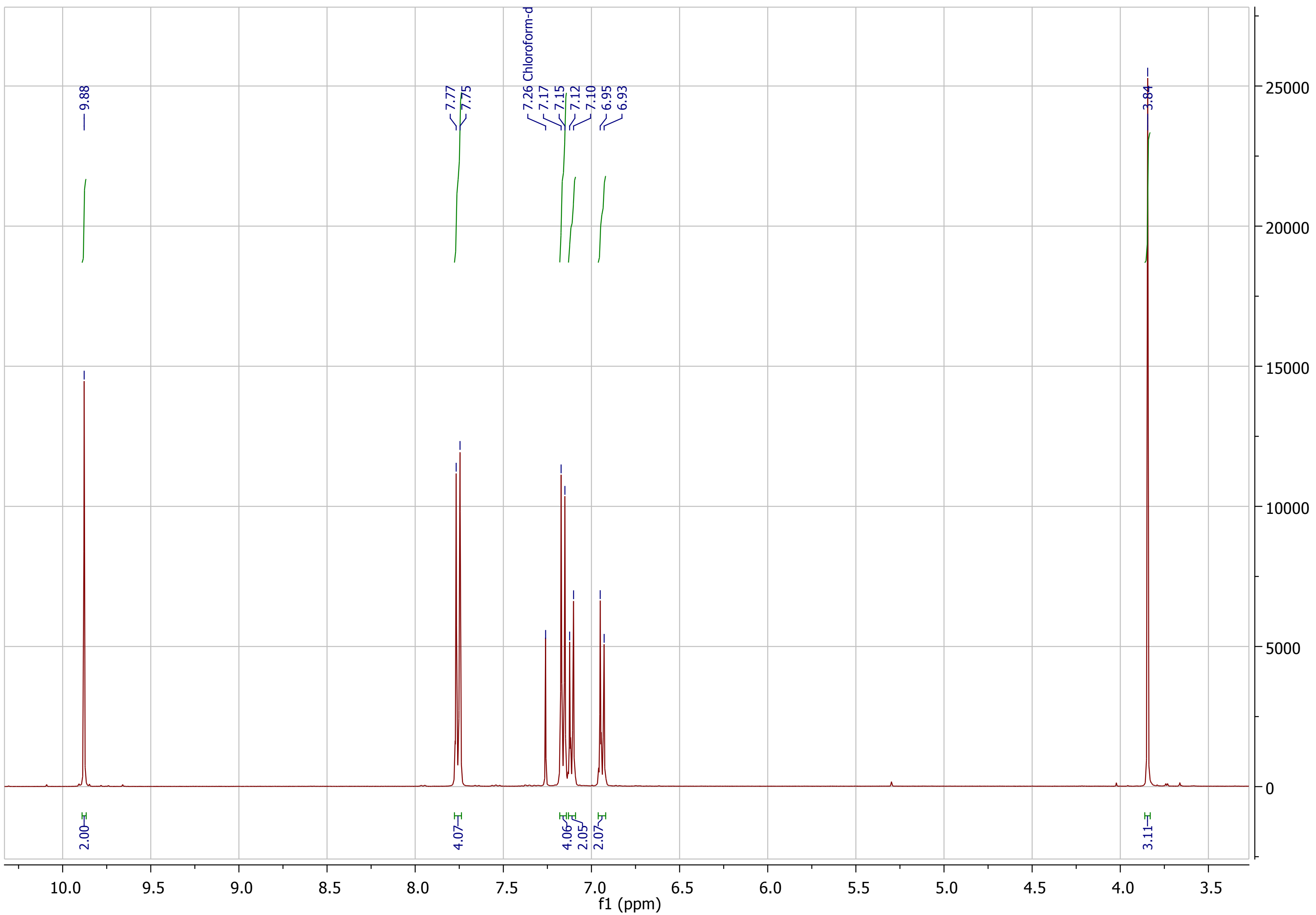

Figure S40 ^{1}H NMR spectrum of **2**.

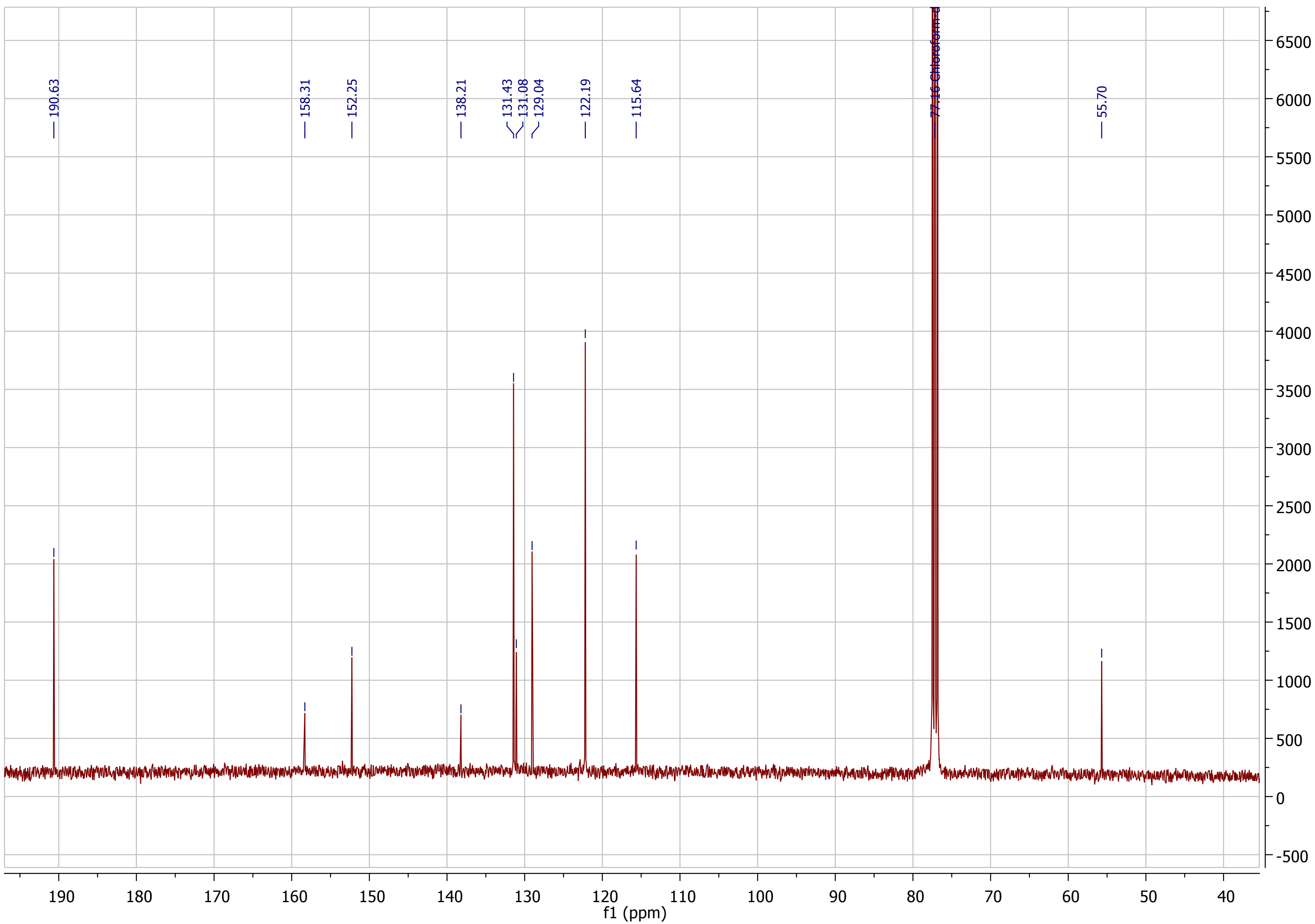

Figure S41. ^{13}C NMR spectrum of **2**.

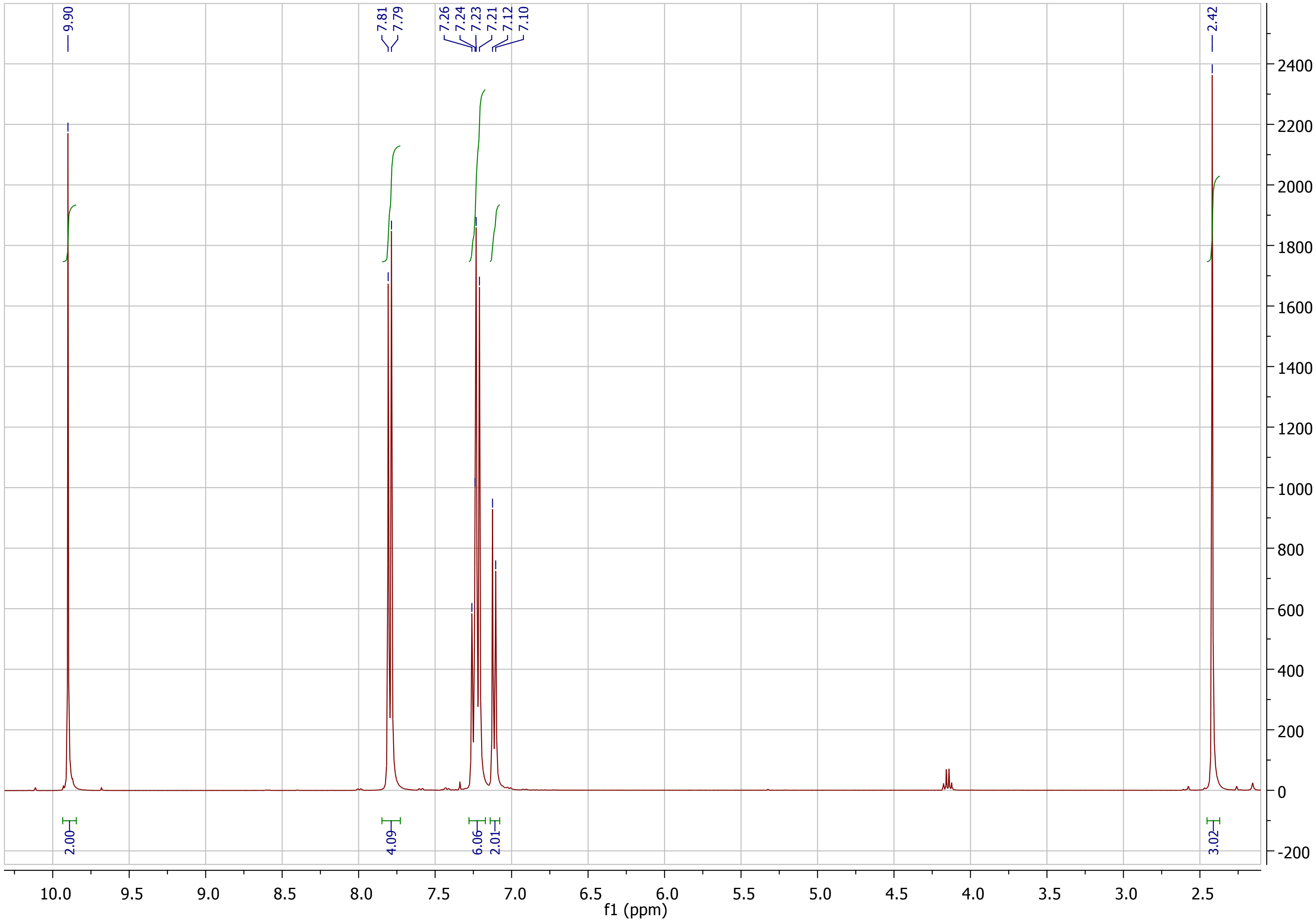

Figure S42. ^{1}H NMR spectrum of **3**.

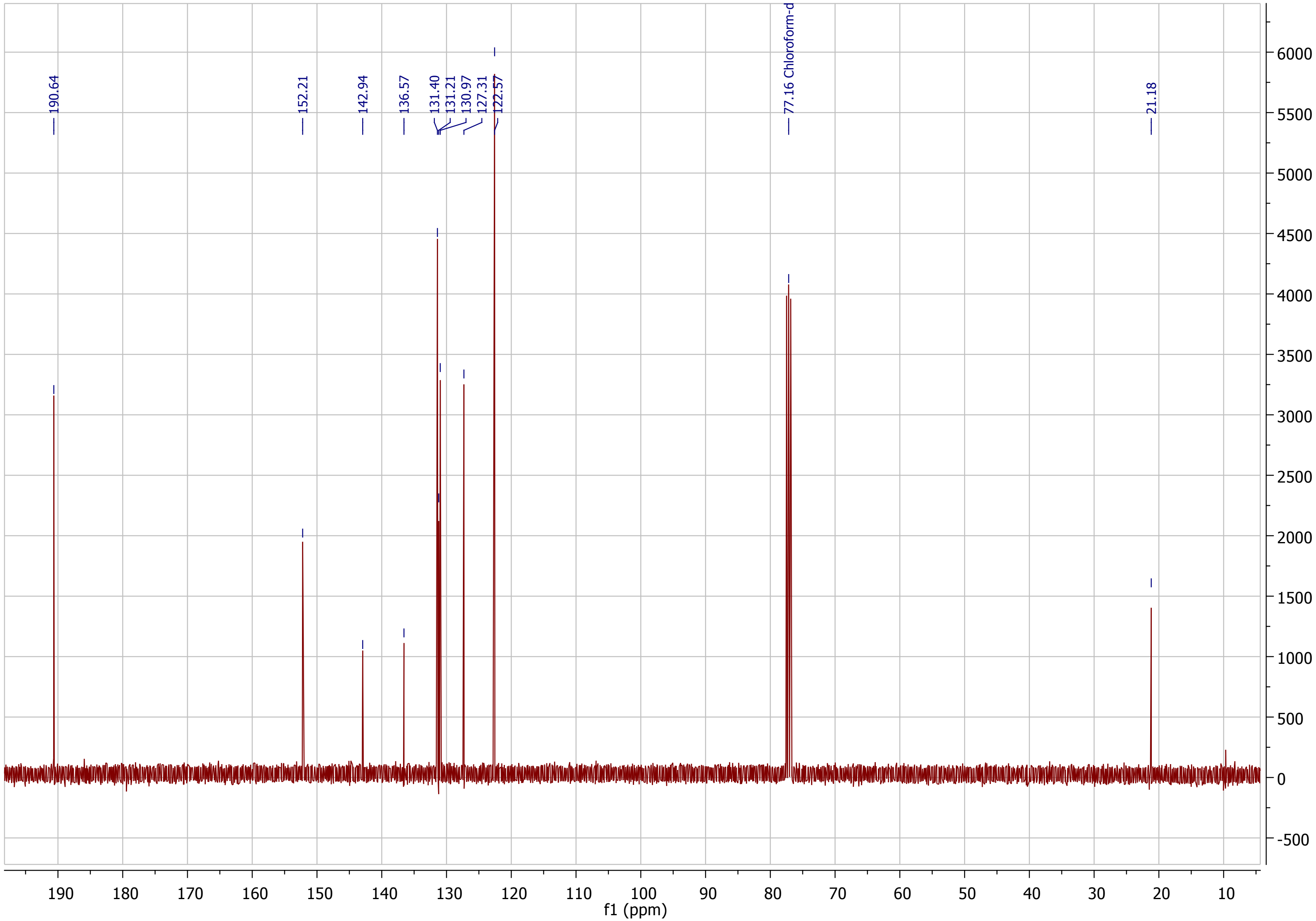

Figure S43 ^{13}C NMR spectrum of **3**.